

Mountain-building in Taiwan: a thermo-kinematic model

Martine Simões ^{1,2}, Jean Philippe Avouac ¹, Olivier Beyssac ², Bruno Goffe ², Ken Farley ¹, Yue-Gau Chen ³

¹ Tectonics Observatory, California Institute of Technology, Pasadena, USA.

² Laboratoire de Géologie, Ecole Normale Supérieure, Paris, France.

³ Department of Geosciences, National Taiwan University, Taipei, Taiwan (R.O.C.)

To be submitted to Journal of Geophysical Research

Abstract

Taiwan is a case example of a collisional orogen. This example has inspired in particular the most popular critical wedge model of mountain-building. This model seems irreconcilable with available data on the metamorphic history of the range, including new data from peak metamorphic temperatures measured from RSCM thermometry and (U-Th)/He cooling ages. In addition it seems that most of (if not all) the ~39.5 to 44.5 mm/yr of shortening across the range are taken up by localized thrusting on the major frontal faults within the western foothills. This is also in contrast with the previous idea that the prism would undergo distributed shortening so as to maintain its critical taper. These various data are used here to develop an alternative thermo-kinematic model of the Taiwan orogen. In this model, the pre-Tertiary basement within the Tananao Complex has been uplifted as a result of sustained underplating at the base of the wedge and has been exhumed at a rate of ~6.3 mm/yr, with no significant diachronism from north to south; the flux of underplated material beneath TC seems to have increased significantly ~ 1.5 Ma ago. The Hsueshan Range, further west, is another area where sustained uplift due to underplating is taking place with uplift rates of ~4.2 mm/yr. In between these two domains the Backbone Range is thrust westward along the detachment connecting these two underplating windows, and experiences moderate exhumation of the order of 0.4 mm/yr. In the model, the topography is assumed steady-state and the flux of crust eroded away is balanced essentially by underplating beneath the TC and HR. Presently, frontal accretion does not account for more than ~10% of the incoming flux into the orogen, although there is indication that this term may have been much larger (~80%) before about 1.5 Ma ago. A significant amount (~70 %) of the underthrust crust of the Chinese continental margin ends up being subducted

east of the Longitudinal Valley and Coastal Range, probably because of an increase in crustal density at depth. We also show that the density distribution resulting from metamorphism within the orogenic wedge may be a key factor explaining the topography of the range. This study thus sheds new light onto the processes involved in the young arc-continent collision of Taiwan.

1. Introduction

The Taiwanese range is an ideal place where to investigate mountain-building processes due to its high rates of crustal deformation and erosion. In addition to that, the collision of the Chinese continental margin with the Luzon volcanic arc (figure 1), that initiated ~6.5 Ma ago in the north (eg. [Lin, *et al.*, 2003]), has been since been propagating to the south because of the obliquity in the geometry of the two plates involved [Byrne and Liu, 2002; Simoes and Avouac, in prep.; Suppe, 1981, 1984]; consequently, this orogen also offers a unique opportunity to investigate the temporal evolution of a young active mountain belt by looking at different transects across the range, from south to north. The example of Taiwan has also proved key in the development of the popular and well-accepted critical wedge model of mountain-building [Barr and Dahlen, 1989; Barr, *et al.*, 1991; Chapple, 1978; Dahlen and Barr, 1989; Davis, *et al.*, 1983], which holds that a range undergoes distributed deformation, so as to maintain a self-similar geometry dictated by the internal friction angle of the medium and the shear stresses at the base of the wedge. In fact, the kinematics of deformation of the Taiwan orogen, crucial to test mountain building models, remains poorly constrained.

The orogen has been relatively well-documented in terms of structural geology of the range [Clark, *et al.*, 1993; Crespi, *et al.*, 1996; Faure, *et al.*, 1991; Fisher, *et al.*, 2002; Ho, 1986, 1988; Pulver, *et al.*, 2002; Tillman and Byrne, 1995], metamorphism [Beysac, *et al.*, in prep.; Ernst, 1983; Ernst and Jahn, 1987] and thermo-chronology [Beysac, *et al.*, in prep.; Liu, *et al.*, 2001; Lo and Onstott, 1995; Willett, *et al.*, 2003]. Also, by analyzing the foreland basin and recent deformation across the Western Foothills, [Simoes and Avouac, in prep.] have been able to quantify the long-term shortening rate across the range (figure 1); however, this study questions the applicability of the critical wedge theory to Taiwan by suggesting that the range would undergo little, if any, internal deformation. In addition, a wealth of data on peak metamorphic temperatures and (U-Th)/He low temperature thermochronology across the slate belt of Taiwan, has been recently produced [Beysac, *et al.*, in prep.], and seems inconsistent with the thermal

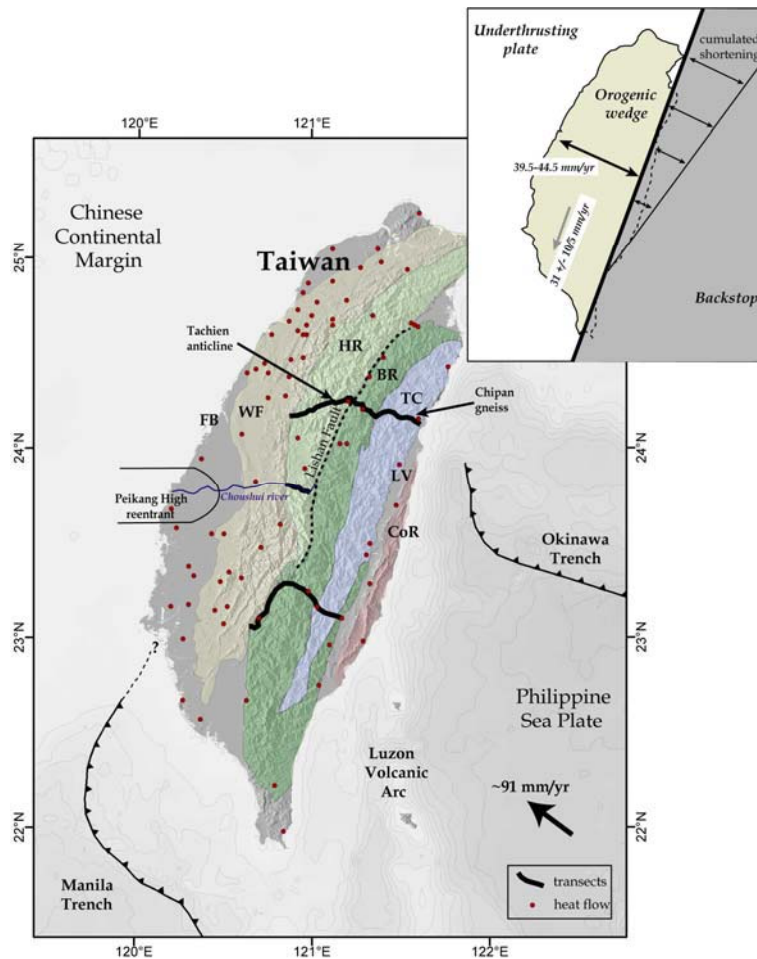
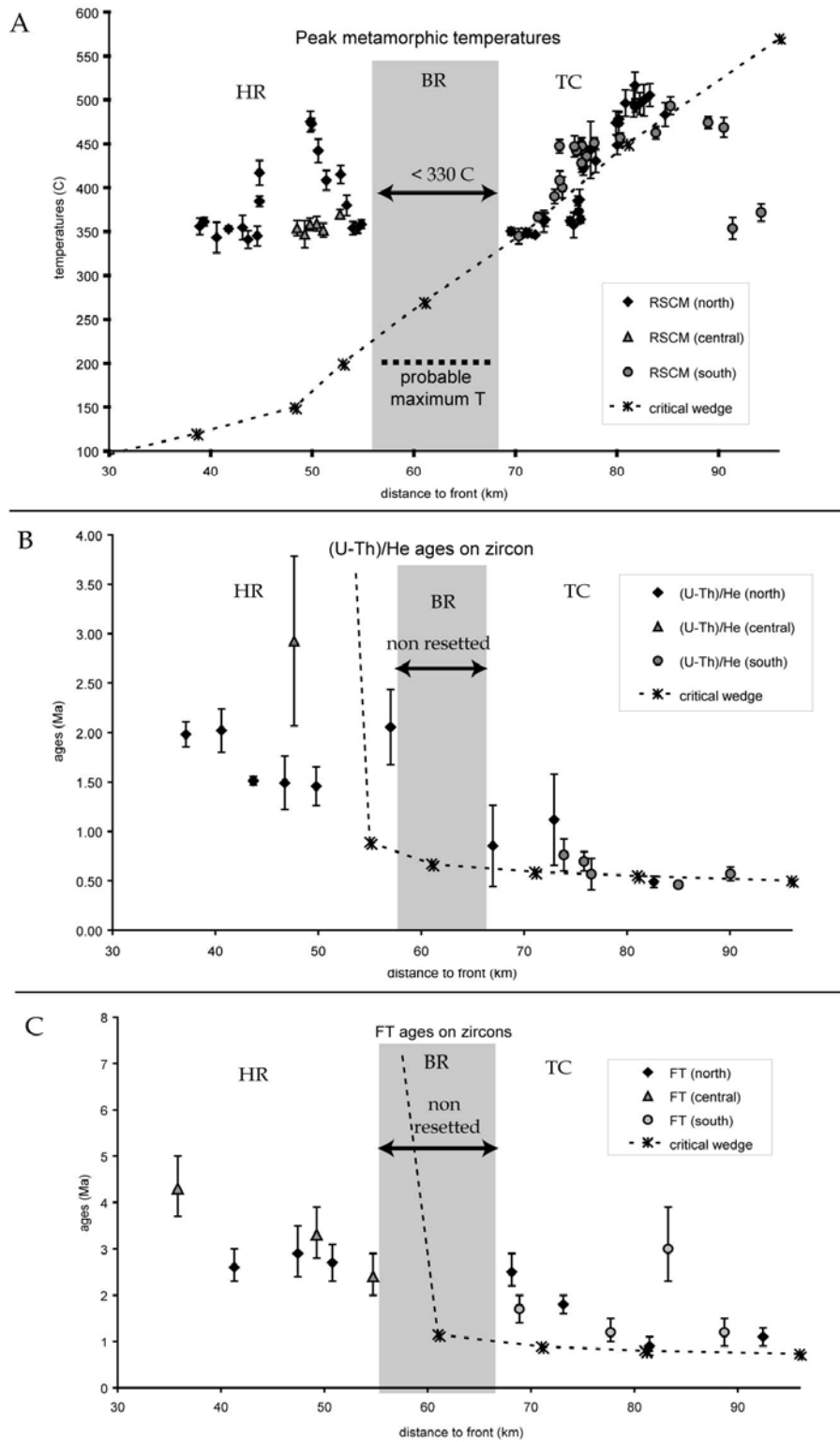


Figure 1: Geodynamical and geological context of Taiwan. The plate boundary here is complex because of the presence of two subduction zones of reverse polarities, accommodating the rapid convergence between the Philippine Sea plate and the Eurasian plate [Sella, et al., 2002]. Our study area is the central portion of Taiwan where the collision between the Luzon Volcanic Arc and the Chinese continental margin took place since 6.5 Ma ago (e.g. [Lin, et al., 2003]). Because of the obliquity in the direction of these two structures, the collision has been propagating to the south where the orogen is less mature. This is rather useful in studying the temporal evolution of the Taiwanese range through different sections; indeed, our study mostly focused on the thermal state along three sections well-documented in terms of structural geology, thermometry and thermo-chronology. For reference the main structural domains in Taiwan are reported: from west to east, the foreland basin (FB), the Western Foothills (WF), the Hsueshan Range (HR) separated from the Backbone Range (BR) by the Lishan Fault, the Tananao Complex (TC), the Longitudinal Valley (LV) and the Coastal Range (CoR). The two latter ones are of Philippine Sea Plate affinity and may be considered as the backstop of the range (inset). Also indicated in the inset are the southward migration rate of maturation of the range and the shortening rate accommodated across the orogenic prism [Simoes and Avouac, in prep.]. Heat flow data are from [Lee and Cheng, 1986].

evolution predicted from the critical wedge theory [Barr and Dahlen, 1989] (figure 2). Our study aims at integrating these recent findings to reappraise the thermo-kinematic evolution of the Taiwanese range; this is key in understanding mountain-building processes since the thermal state of the orogen results from the interplay between kinematics of deformation and erosion, and most certainly exerts a major control on



(Figure 2)

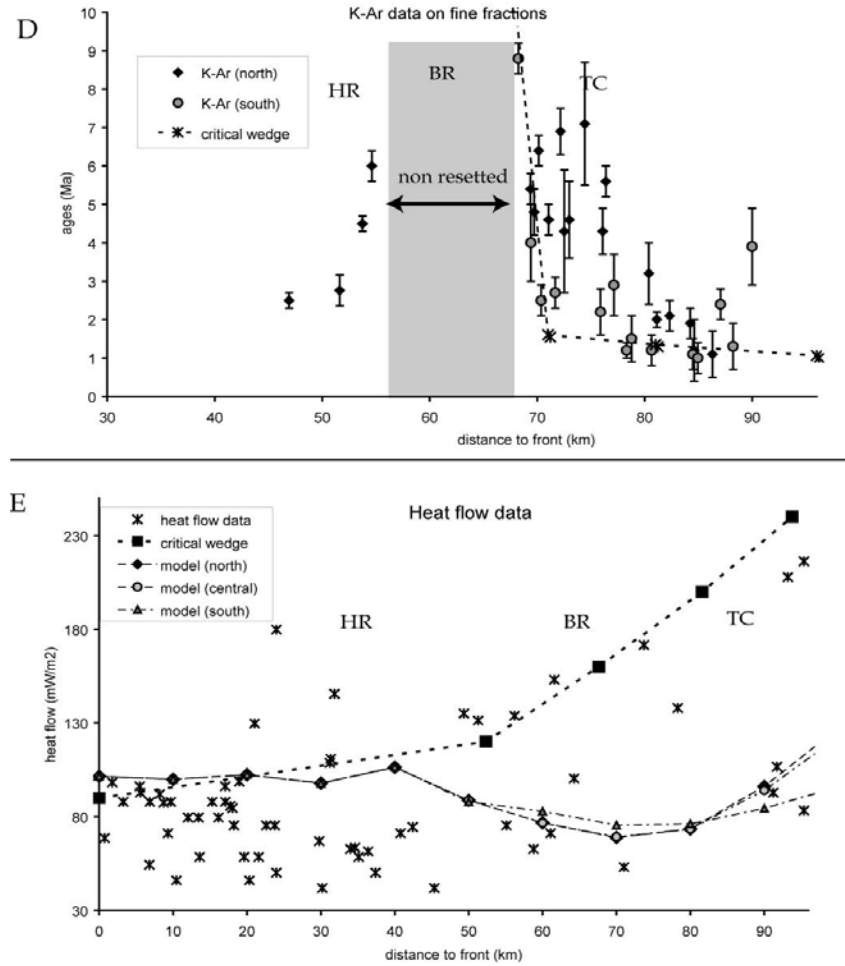


Figure 2 (this and previous page): Thermometric, thermo-chronologic and heat flow data for the three transects represented in figure 1, as well as the predictions from the thermo-kinematic model of [Dahlen and Barr, 1989] and [Barr and Dahlen, 1989] for the maximum rate of 25 % of underplating that they proposed. The shaded area locates the common portion of the range where RSCM peak temperatures are below the resolution limit of 330 °C [Beysac, et al., 2002], and where cooling ages are partially resetted. HR: Hsueshan Range – BR: Backbone Range – TC: Tananao Complex. 2-σ error intervals were represented. (A) Peak metamorphic temperatures retrieved from the RSCM method [Beysac, et al., in prep.]. Data below the 330°C resolution limit were not represented for lisibility; although the exact peak temperatures over the BR may not be retrieved by this technique, partially resetted (U-Th)/He ages on zircon in this domain indicate that the rocks have probably not been submitted to temperatures higher than 200 °C. Major north-south changes may be essentially observed within the HR or structural equivalents. The critical wedge model of [Dahlen and Barr, 1989] and [Barr and Dahlen, 1989] predicts a thermal gradient slightly lower than the one observed over western TC and eastern BR; a higher contribution of underplating would actually allow for fitting this observation. But, more importantly, this model does not account for the exhumation of the HR. (B) (U-Th)/He ages on detrital zircons [Beysac, et al., in prep.] showing young ages within the HR of the central and northern transects, and within the TC; data from the BR were essentially non-resetted or partially resetted. A closure temperature of 180 °C has been used to retrieve the predictions for the critical wedge model. (C) χ^2 fission-track (FT) ages on detrital zircons from [Liu, et al., 2001]; data from [Tsao, 1996] were not shown here since they show a consistent pattern. A closure temperature of 240 °C was considered for model predictions. (D) K-Ar ages on white micas fine fractions [Tsao, 1996]; a closure temperature of 300 °C, instead of 350 °C, is considered. (E) Heat flow data [Lee and Cheng, 1986] over the whole width of the range (figure 1); values higher than 250 mW/m² and lower than 30 mW/m² were not represented since they are most probably related to ground water circulation [Song and Ma, 2002]. Also shown is the heat flow predicted by the critical wedge model and our final results for the three transects of figure 1. The scatter of the data is such that no overall trend may be realistically retrieved; the critical wedge model of [Dahlen and Barr, 1989] and [Barr and Dahlen, 1989] predicts heat flows in the highest acceptable values over the TC, while our preferred models are closer to the minimum values.

crustal deformation and thus on particle trajectories through the temperature-dependent rheological properties of rocks (e.g. [Avouac and Burov, 1996; Beaumont, et al., 1992; Cattin and Avouac, 2000; Godard, et al., 2004; Koons, 1990; Koons, et al., 2002; Willett, 1999; Zeitler, et al., 2001]). In this study we will follow the modeling approach of [Henry, et al., 1997] and [Bollinger, et al., subm.]. The kinematics is prescribed and we then solve for the time evolution of the thermal structure. This makes it possible to compute PT-t paths and adjust the model to thermometric and thermo-chronological data.

Hereafter, we first present the structural, thermometric and thermo-chronological data used in this study and investigate how previous models of the Taiwan orogen fail in reconciling all these observations; our proposed scenario as well as our modeling approach are subsequently explained. It appears from our study that the metamorphic evolution of the pre-Tertiary basement has been almost synchronous from north to south, while further west the western portion of the slate belt shows the greatest spatio-temporal variations in growth and maturation. By combining the thermo-kinematics derived for these different units, we are able to reconcile successfully the overall evolution of the orogen, and to propose thermal structures on three transects across Taiwan. We find that no internal shortening is needed within the wedge to account for the metamorphic and structural history of the range, which is in contrast with the critical wedge model applied to Taiwan in the past. Our study also allows for reappraising the contribution of underplating to mountain-building relatively to frontal accretion, and for quantifying a kinematic framework at the crustal scale, with the involved fluxes of material, based on the derived long term erosion rate averaged over the whole range.

2. Geological context and constraints on the thermo-kinematic evolution of the range.

2.1 Tectonic background.

Details regarding the structural and stratigraphic setting of our study area are presented by [Beyssac, et al., in prep.]; here we just provide an overview of the main tectonic provinces illustrated in figure 1. Taiwan results from the southward propagating collision between the Luzon volcanic arc and the Chinese continental margin, which converge at a rate of ~90 mm/yr in a NW direction according to the REVEL

plate model [Sella, *et al.*, 2002] (figure 1). Along the east coast of the island, the Coastal Range (CoR) of Luzon arc affinity, and the Longitudinal Valley (LV) which marks the suture between the Eurasian and Pacific plates, may be both considered as the backstop of the Taiwanese range (e.g. [Simoes and Avouac, in prep.]). The most internal and metamorphosed portion of the range is exposed within the Tananao Complex (TC) and is constituted of highly deformed pre-Tertiary basement (e.g. [Faure, *et al.*, 1991; Pulver, *et al.*, 2002]). It is stratigraphically overlain by the Eocene to Miocene meta-sediments of the slate belt, originally deposited on the passive margin during rifting and opening of the South China Sea (e.g. [Ho, 1986, 1988]). The eastern portion of this belt, the Miocene and Eocene Backbone Range (BR) indicates an overall top-to-the-west sense of shear, as in the adjacent basement, but with a less intense pervasive deformation [Clark, *et al.*, 1993; Fisher, *et al.*, 2002; Tillman and Byrne, 1995]; the western TC-eastern BR ensemble appears as a stratigraphically inverted series. In contrast, the western portion of the slate belt, the Eocene to Oligocene Hsueshan Range (HR), separated from the BR by the Lishan fault (figure 1), shows only coaxial deformation with simple folding and no overturning of the thick sedimentary sequences [Clark, *et al.*, 1993; Tillman and Byrne, 1995]; balanced cross-sections suggest this domain has been emplaced by brittle duplexing of discrete thrust sheets [Powell, 2003]. The HR has actually been interpreted as a past half-graben that had been accreted to the range [Clark, *et al.*, 1993; Lee, *et al.*, 1997; Tillman and Byrne, 1995]. Exhumation of these meta-sediments within the HR culminates at the level of the Eocene Tachien anticline (e.g. [Beysac, *et al.*, in prep.; Tillman and Byrne, 1995]). Further west, the fold-and-thrust-belt of the Western Foothills (WF) consists of non-metamorphic syn-orogenic sediments previously deposited in the adjacent foreland basin of Taiwan. An overall thin-skin tectonics style may be proposed for this area (e.g. [Suppe, 1980b, 1987]); however, to the south deformation may be more complex (e.g. [Hickman, *et al.*, 2002; Hung, *et al.*, 1999; Mouthereau, *et al.*, 2001; Suppe, 1980a]), and it has been proposed that the most internal complex portions of the south WF would be younger structural equivalents to the HR further north [Simoes and Avouac, in prep.]. All the thrust faults along the western foothills root to a common decollement at a depth of about ~5km (e.g. [Yue, *et al.*, 2005]) and it has been suggested that this decollement can be traced beneath the Central Range (CR) from background micro-seismicity [Carena, *et al.*, 2002]. Finally, because of the slight obliquity between the direction of transport and the structural trend in Taiwan, left-lateral shear is ubiquitous over the range (e.g. [Faure, *et al.*, 1991; Pulver, *et al.*, 2002]).

2.2 Heat flow data

Some surface heat flow measurements have been performed across the range by [Lee and Cheng, 1986] (figure 1), although arguable because some of the boreholes are only 100 to 200 m deep and thus potentially affected by the effects of temperature changes at the surface (e.g. [Turcotte and Schubert, 2002]). Some extremely low ($<30 \text{ mW/m}^2$) and high values ($>250 \text{ mW/m}^2$) most probably correspond to hydrothermal areas perturbed by ground-water circulation [Song and Ma, 2002], and were thus excluded from our analysis. Overall, although surface heat flow has been previously seen as generally increasing from $\sim 80 \text{ mW/m}^2$ in the Coastal Plain to $\sim 240 \text{ mW/m}^2$ within the basement of the TC, the scatter in the values on all transects (figure 2) may not allow for deriving an accurate pattern; also, coverage on the HR domain, critical to our modeling, is rather sparse (figure 1). These data have been extensively used to test previous thermal and thermo-kinematic models of the Taiwanese range; however, since they most certainly do not provide the tightest constraints on the thermal evolution of the orogen, we will not give them too much weight in our analysis.

2.3 Petrologic, thermometric and thermo-chronometric constraints.

As reviewed in more details by [Beyssac, *et al.*, in prep.], petrologic constraints are rather scarce throughout most of the Central Range (CR) of Taiwan since the mineralogy of the slates (HR and BR) is not suited for conventional petrologic investigations; they have hypothesized that this poor mineralogy is the consequence of the overall chemistry of the rocks, as well as of potential kinetic limitations due to the extremely fast processes involved in this orogeny. However, some studies of the basement complex to the east have yielded metamorphic conditions for the blueschist exotic blocks in the Juisui area ($\sim 450\text{-}500^\circ\text{C}$, $>7 \text{ kbar}$) [Ernst and Jahn, 1987; Liou, *et al.*, 1975] that are Cenozoic in age [Lo and Yui, 1996] [Ernst and Jahn, 1987]; whether or not these blocks had a metamorphic history similar to the schists present within the basement is not clear (e.g. [Beyssac, *et al.*, in prep.]).

Some crucial data on peak metamorphic temperatures encountered by these rocks in both the slate belt and the TC have been recently provided by the Raman spectroscopy of carbonaceous material (RSCM method), which is a major constituent of the slates and schists [Beyssac, *et al.*, in prep.]. These data indicate an inverted thermal gradient within the western TC and eastern BR, across both the central and southern cross-island highways, with temperatures decreasing from ~ 500 to less than 330°C westward

(Figure 2). While maximum temperatures do not exceed 330 °C within the BR, RSCM on the slates of the HR documents a normal thermal gradient within the easternmost portion of this structure, with temperatures increasing from ~350 °C along the Lishan lineament to 475 °C within the Tachien anticline (figure 1). This high temperature is most probably inherited from the rifted passive margin [Beyssac, *et al.*, in prep.] and requires exhumation of quite deep structural levels. Across the southern termination of the HR, along the Choushui river (figure 1), temperatures are nearly uniform around 350-370 °C [Beyssac, *et al.*, in prep.] (figure 2).

Thermo-chronologic data also provide useful constraints on the cooling history of rocks up to the surface. ^{40}Ar - ^{39}Ar ages on biotite for the Chipan gneiss in the TC [Lo and Onstott, 1995], as well as K-Ar data on white micas fine (< 2 μm) fractions [Tsao, 1996] across the main transects of the range would document the higher temperature history of this cooling. However, the quality (for the data from [Tsao, 1996]) and significance (for [Lo and Onstott, 1995]) of these data may be arguable, and closure temperatures for the K-Ar ages may be as low as 250 °C [P. Renne, pers. comm.]. Fission tracks (FT) on detrital zircons [Liu, *et al.*, 2001; Tsao, 1996] across the two main cross-island highways of Taiwan reveal very young ages within the TC and HR, whereas the BR does not show ages reset by the present orogeny (figure 2); because of the dispersion observed in the ages retrieved from different grains on the same sample, χ^2 ages will be considered for the data set from [Liu, *et al.*, 2001]. The overall pattern of young ages within the TC and HR, and of partially reset data within the BR is also confirmed and refined from recent (U-Th)/He ages on detrital zircon along the same transects [Beyssac, *et al.*, in prep.] (Figure 2). (U-Th)/He and FT ages on apatites [Beyssac, *et al.*, in prep.; Willett, *et al.*, 2003] will not be used here because they are most sensitive to surface conditions and because they mostly were sampled along the complex suture in eastern CR. When thermo-chronologic data are used to constrain any thermal model, some caution has to be taken regarding the choice of the closure temperatures. Indeed, these temperatures may be dependent on the thermal history of the particles. Values of 230-260 °C may be proposed for the FT on zircon [Liu, 1982; Liu, *et al.*, 2001]; in the case of (U-Th)/He dating on zircon, a closure temperature of 180 °C is usually assumed (e.g. [Reiners, *et al.*, 2004]) but we will subsequently consider a possible range of temperatures between 150 to 180 °C.

Finally, peak metamorphic temperatures derived from the RSCM method as well as the (U-Th)/He ages on zircon provide the most reliable constraints. Altogether this dataset shows a consistent picture with exhumation rates higher within the TC and HR, than within the BR (figure 2); also, partially reset thermo-chronometric ages put some constraints on the maximum temperatures encountered by the rocks

within the BR, where RSCM data only indicate temperatures below the 330 °C resolution limit of the method [Beyssac, et al., 2002]. The basement complex does not show any major evolution from north to south, whereas the westernmost HR to the north appears to have been submitted to much more exhumation than its structural equivalents to the south (figures 2 and 3).

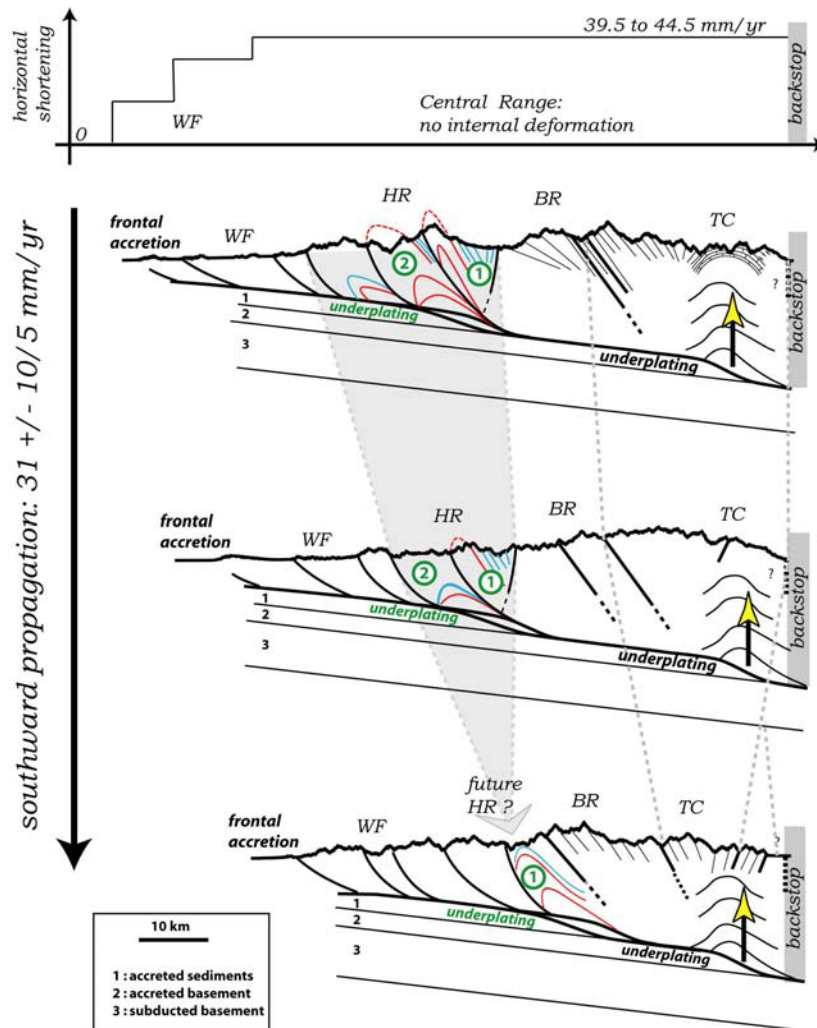


Figure 3: Kinematic and tectonic scenario modeled in this study. The cross-sections along the three transects represented in figure 1 (top to bottom: from north to south), and the locations of probable underplating are taken from [Beyssac, et al., in prep.]. Horizontal shortening and the southward propagation rates are given after [Simoes and Avouac, in prep.]; note that the southward migration rate should mostly apply to the emplacement of the HR. See text for more details.

2.4 Kinematic framework

Some insights into the kinematics of deformation across the Taiwanese range have been gained from the analysis of the foreland basin [Simoes and Avouac, in prep.]. A long-term shortening rate across the range

of 42.0 +/- 2.5 mm/yr (figures 1 and 3) has been estimated from sediment progradation over the foreland basin. This deformation appears to be mostly accommodated across the active frontal faults within the WF, which suggests that the orogenic wedge is submitted to little, if any, internal deformation. In addition to that, the spatio-temporal distribution of syn-orogenic sedimentary depot-centers indicates a $31 \pm 10/5$ mm/yr of north-south propagation of orogenic growth (figures 1 and 3), which is most probably related to the emplacement of the HR; the present location of highest subsidence and thus of maximum orogenic growth would be at the latitude of the Choushui river (figure 1), which is consistent with the less evolved structures in the WF south of this river. This southward propagation rate can be used to relate different transects across Taiwan to different temporal stages of evolution of the range, and more particularly of the HR. By taking into account the long-term shortening rate, the distance-to-time equivalence from the southward propagation rate, as well as the lateral variations in the width of the range, [Simoes and Avouac, in prep.] were able to estimate the thickness of the slice of underthrust crust that is incorporated into the orogenic wedge as a function of the average erosion rate. This analysis requires some amount of crustal subduction which remains not well constrained given the wide range of estimated erosion rates [Dadson, et al., 2003; Willett, et al., 2003].

2.5 Previous thermal models of Taiwan.

Various models of the thermal structure of the range have been proposed in the literature. A popular thermo-kinematic model is based on the critical wedge theory [Barr and Dahlen, 1989; Barr, et al., 1991]. It assumes that the range mostly grows by frontal accretion and that it undergoes distributed shortening so as to maintain a constant topographic slope; underplating has been considered but these authors concluded that it could only be a minor contribution to incoming fluxes (<10-25 %). The model was found to provide a reasonable fit to the heat flow data as well as to the eastward increase of metamorphic grade across the range [Barr, et al., 1991]. Their model assumed a total shortening rate of 70mm/yr across the orogen, too high in light of the ~42 mm/yr derived from the development of the foreland basin [Simoes and Avouac, in prep.], and was assuming a stationary thermal structure neglecting the possibility of lateral and temporal variations. The main problem with this model is that it can not account for the high peak temperatures and young cooling ages in the HR (figure 2). Indeed, the high inverted thermal gradients retrieved from RSCM data across the western TC and eastern BR (figure 2) suggest a contribution of underplating greater than previously thought.

[Hwang and Wang, 1993] questioned the continuous model of [Barr and Dahlen, 1989; Dahlen and Barr, 1989] by investigating the effects of discrete sequential thrusting on the thermal structure of the range; however this model was only tested in light of the heat flow data. Later on, following a model of crustal subduction with subsequent rapid exhumation of the Central Range (CR) [Lin, 1998], [Lin, 2000] proposed a thermal model mainly adjusted to fit the heat flow data as well as the gap of seismicity within the CR. This model accounts for underplating below the TC but neglects lateral and vertical advection of heat; it also assumes steady state. Another 1D-model has been proposed by [Song and Ma, 2002], and accounts for crustal thickening and erosion. Finally, to estimate the rheological properties of the range and foreland system, [Zhou, et al., 2003] reviewed possible values for thermal parameters and discussed the effects of a thinned lithosphere on the strength across the range. None of these more recent models has been tested in view of the thermo-chronological and metamorphic data.

2.6 Proposed scenario of emplacement of the range.

Altogether, by integrating structural, thermometric and thermo-chronologic data, [Beyssac, et al., in prep.] proposed a possible tectonic scenario for the evolution and emplacement of the Taiwanese range, that can be combined with the findings of [Simoes and Avouac, in prep.] (Figure 3). Qualitatively, the structure of the range, its metamorphic organization and the thermo-chronological data suggest that growth of the wedge most probably resulted from a combination of underplating beneath the TC, brittle duplexing within the HR and some frontal accretion along the WF. The 42 ± 2.5 mm/yr of total shortening across the range has been mostly accommodated across the major frontal faults of the WF [Simoes and Avouac, in prep.]; over the long-term, the range would have then been mostly growing without much internal shortening (figure 3). An analogous scenario has been actually already proposed recently for the Himalayas of central Nepal [Bollinger, et al., 2004a; Bollinger, et al., subm.]. The HR shows the most significant north-south variation: to the south it is still most probably buried beneath the BR and the complex southern WF, while to the north exhumation has been much more intense and the structure appears to be much more mature [Beyssac, et al., in prep.; Simoes and Avouac, in prep.] (figure 3). The $31 \pm 10/5$ mm/yr of southward orogenic growth proposed by [Simoes and Avouac, in prep.] is thus most probably related to the HR.

The scheme of figure 3 will be the basis for the thermo-kinematic model proposed in this study. Note that we do not attempt to account for the range north of the central cross-island highway (northern transect in

figure 1), since the reversal of the subduction polarity at the Ryukyu Trench and backarc extension most probably affects crustal deformation.

3. Modeling set up.

3.1 Modeling approach.

We chose to model the thermo-kinematics of Taiwan by using the 2D finite-element program FEAP, developed by R. Taylor of U.C. Berkeley (USA), and modified by P. Henry (CEREGE, France) [Henry, *et al.*, 1997]. This code allows for solving the transient thermal evolution of the range, and is most appropriate for our case study since it accounts for erosion, and since the kind of kinematics we propose can be implemented.

The heat equations account for diffusion, advection and internal heat sources such as radiogenic heat production and shear heating along the main basal shear zone; they are solved within an Eulerian frame [Zienkiewicz and Taylor, 1989]. Shear heating is computed from the thickness and the velocity discontinuity across the shear zone, as well as the shear stress. This latter depends on the assumed friction coefficient, as well as the lithostatic pressure computed from the petrogenetic grid of [Bousquet, *et al.*, 1997] (see [Henry, *et al.*, 1997] for more details on this computation). A flow law, depending on the strain rate and the material properties, is assumed for the ductile regime. Parameters used to compute lithostatic pressures and shear heating are summarized in tables 1 and 2.

The details of the kinematics and thermal structure in the WF are ignored because it does not affect the prediction of the model regarding the structure and P-T-t paths below the more internal part of the range. Underplating and accretion may be modeled as continuous processes by allowing material transfer through the basal shear zone, across an underplating window where non-coaxial deformation may be acquired by the rocks (figures 4 and 5). Computation of peak temperatures and cooling ages by particle tracking through the time-dependent thermal field has been also made possible by the modifications of L. Bollinger (CEA, France) [Bollinger, *et al.*, *subm.*].

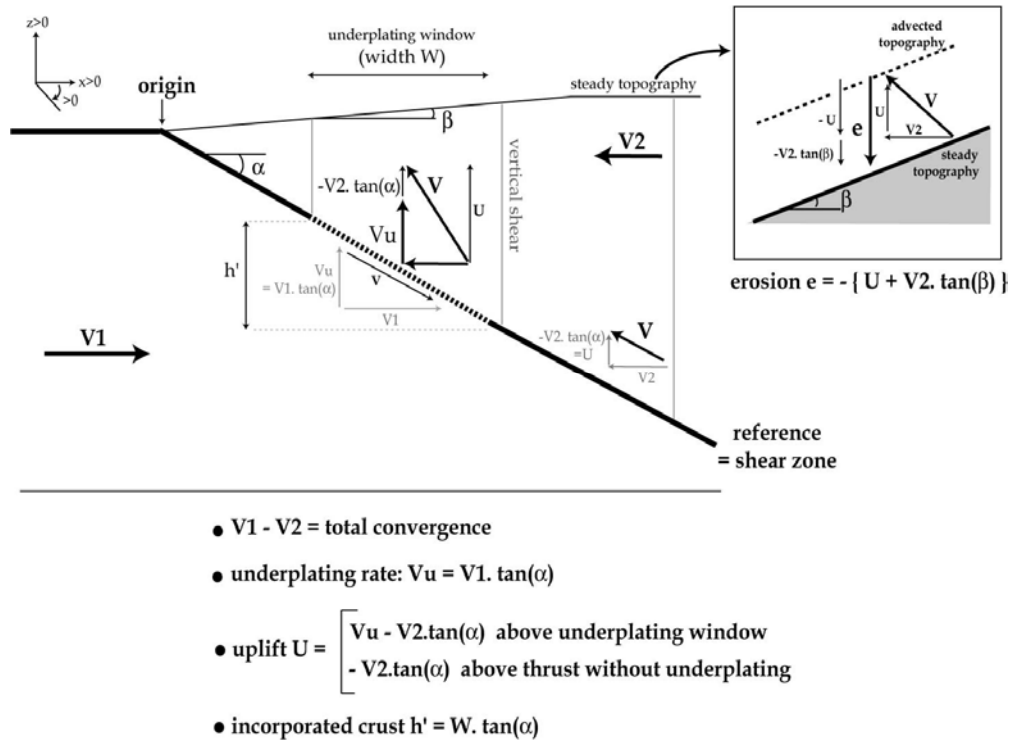


Figure 4: Geometrical and kinematic concepts of the FEAP finite-element program. The basal shear zone of the orogen is taken as the reference, and its intersection with the topographic surface as the origin of the modeling. Horizontal components of underthrusting ($V1$) and overthrusting ($V2$) rates are kept constant within the footwall and hanging walls respectively; conservation of the velocity field is allowed by vertical shear, only represented here in the hanging wall, although also applicable to the footwall. Since topography is assumed to be steady state, modeled erosion e has to balance the total rock uplift U as well as the lateral advection $V2$ of the topography (inset). The thickness of the slice of crust h' incorporated into the range may be easily calculated from the dip angle of the shear zone, as well as from the width W of the underplating window. The angle α needed to determine the underplating and uplifting rates has to be corrected for the dip angle of the Moho in the case of the real modeling. See text for further details.

3.2 Geometric and kinematic scheme

The kinematic scheme used in the model is defined in figure 4. The topography is assumed steady-state. As in the configuration of [Huerta, et al., 1998], the reference frame is attached to this basal contact, and the model origin is taken at the intersection of the shear zone with the topographic surface. Velocities are taken positive from west to east in the sense of underthrusting, and upward for the verticals. Dip angles are positive when dipping to the east (to the right in figure 4). The horizontal components of the underthrusting and overthrusting velocities, $V1$ and $V2$ respectively, are constant within the footwall and hanging wall, and $V1-V2$ is the shortening rate across the range (figure 4). To satisfy the continuity equation, vertical shear of both the footwall and hanging-wall is allowed. This is necessary to allow for

Layer	LPM	LPLC	LPUC	shearzone	OP	UPC	UPM
Conductivity (W/m/K)	2.9	2.9	3.35	3.35	3.35	2.9	2.9
Thermal Diffusivity (m².s⁻¹)	10 ⁻⁶						
Radioactivity (μW/m³)	0	0.39	1.7	1.7	1.7	0	0
Chemical composition	Peridotite	Intermediate	granodiorite	granodiorite	granodiorite	gabbro	Peridotite
Density	3.35	2.91	2.76	2.76	2.76	2.94	3.35
Thermal expansion (K⁻¹)	2.4 E-05	2.4E-05	2.4E-05	2.4E-05	2.4E-05	2.4E-05	2.4E-05
Compressibility (Pa⁻¹)	8 E-12	1 E-11	2 E-11	2 E-11	2 E-11	1 E-11	8 E-12

Table 1: Thermal and physical parameters used in our thermo-kinematic modeling. The different layers refer to those represented in figure 6. Conductivity and radioactivity for LPUC, the shear zone and OP were taken from [Lee and Cheng, 1986], and [Chang, 1989; Song and Ma, 2002] respectively; radioactive heat production for the LPLC is from [Zhou, et al., 2003]. Densities were given for each associated composition based on the computations of [Bousquet, et al., 1997]; densities for metasediments and granodioritic compositions are similar. The thermal expansion coefficient is after [Taylor and McLennan, 1985], and the compressibility after [Turcotte and Schubert, 2002]. Thermal expansion and material compressibility were used to recalculate densities and lithostatic pressure with the procedures described in [Bousquet, et al., 1997] and [Henry, et al., 1997].

Brittle mode		Ductile mode		
τ max (MPa)	effective friction	A (MPa.n.s ⁻¹)	n	Q (kJ/mol)
50	0.1	2.512 E-09	3.4	139

Table 2: Parameters used to compute shear heating, using a granite rheology. Flow law parameters are after [Hansen and Carter, 1982].

underplating (figure 4). Indeed, along the underplating window, the footwall initial velocity vector $V1$ partitions into a vertical underplating vector Vu , transmitted to the hanging wall, and a velocity component parallel to the basal thrust; if α is the dip of the basal thrust at this level, then $Vu = V1 \cdot \tan(\alpha)$. Overthrusting of the hanging wall over the shear zone with a horizontal velocity $V2$ implies by itself a vertical component in the particle trajectories of $-V2 \cdot \tan(\alpha)$, which would suggest that total rock uplift U above the underplating window would equal $(V1 - V2) \cdot \tan(\alpha)$. Since we assume steady-state topography, the model implicitly assumes an erosion rate e which depends on the rock uplift U and on the topographic slope β (inset in figure 4).

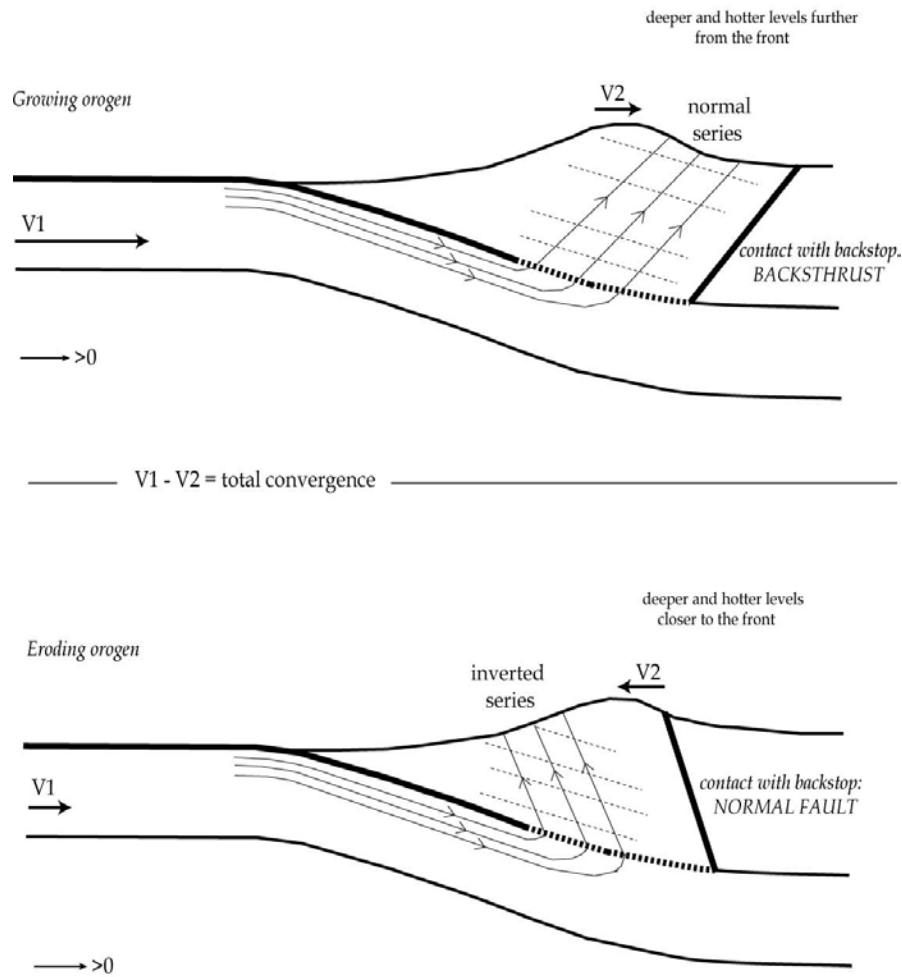


Figure 5: Schematic representation of the implications behind a positive (upper panel) or negative (lower panel) overthrusting rate V_2 . The main differences between these two orogenic modes would lie in the stratigraphic sequence of the series that have been underplated (inverted for $V_2 < 0$ and normal for $V_2 > 0$), the spatial distribution of these series that most probably sample deeper hotter levels of the prism (closer to the front in the case of $V_2 < 0$), as well as the geometry of the contact with the backstop (backthrust for $V_2 > 0$, and normal fault for $V_2 < 0$). In our model, shearing of the rocks would be acquired at the level of the underplating window; dashed lines indicate the shear direction acquired by the rocks that had gone through the underplating window.

3.3 Model geometry and parameters.

A total of six domains of uniform thermal and physical properties (tables 1 and 2, and figure 6) are considered: the mantle, lower and upper crusts of the subducting plate; the orogenic wedge; the mantle and oceanic crust of Pacific plate affinity as the boundary conditions on the eastern side of the system. The mesh of our finite-element model is 10km x 1.5km within the orogenic prism. Because the Chinese passive margin has undergone some extension before the collision, we assume an 80km thick lithosphere

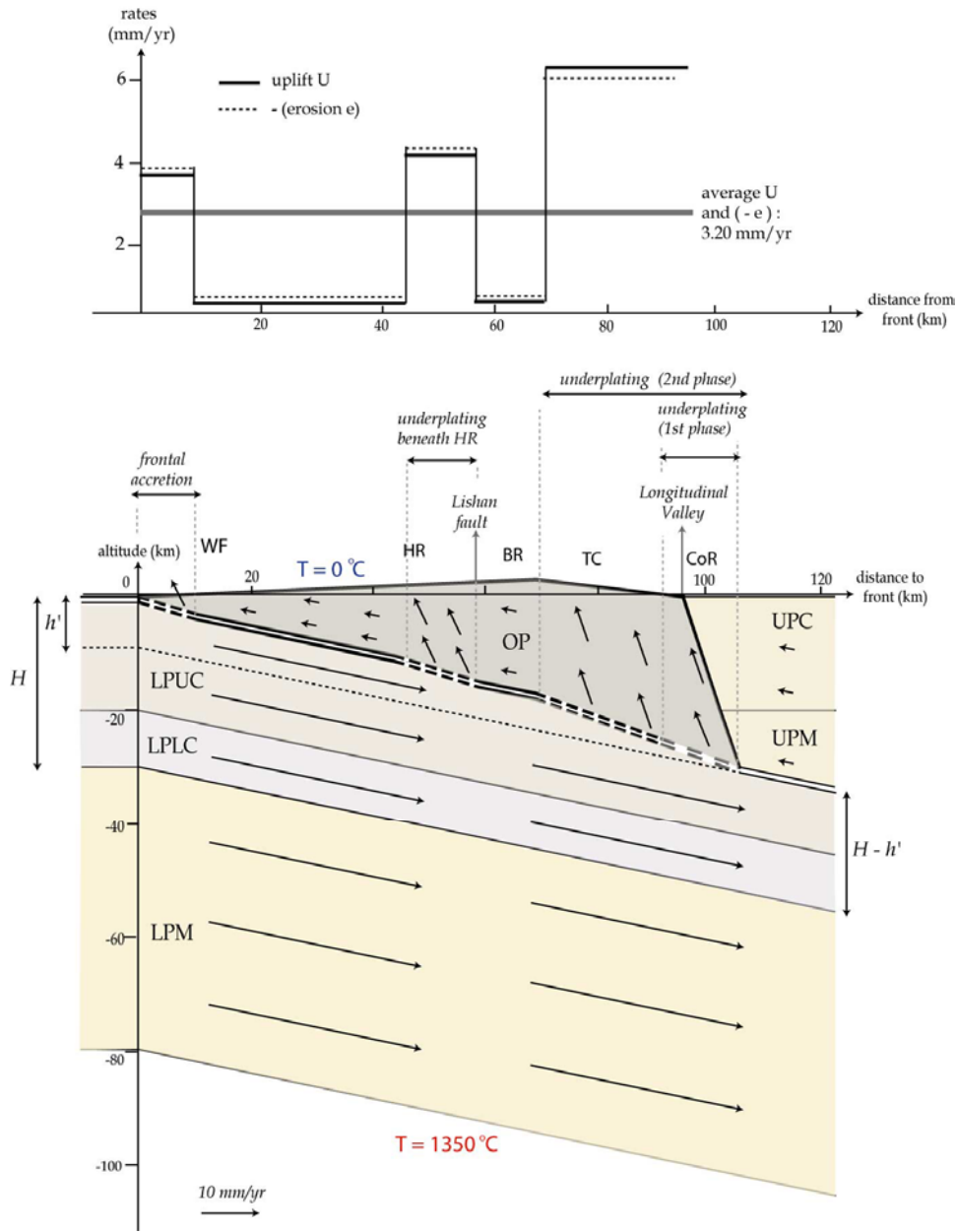


Figure 6: Geometry of our thermo-kinematic model, with the different domains of homogeneous thermal and kinematic properties (table 1): lower plate mantle (LPM), lower plate lower crust (LPLC), lower plate upper crust (LPUC), orogenic prism (OP), upper plate mantle (UPM) and upper plate crust (UPC); the shear zone is represented by a thicker line, which is dashed where the different underplating windows are located. The velocity field as derived from the geometric concepts of FEAP (figure 4) is shown in the case of the most recent phase of underplating below the TC, that prevailed during the last 1.5 Myr. The total thickness H of the Chinese margin crust may be in part integrated into the orogenic prism by frontal accretion and underplating (thickness h' of figure 4); the rest ($H - h'$) would sustain lower crustal thickening not modeled here, and/or be subducted beneath the Philippine Sea plate. The notation h' is here chosen to differentiate from the notation h of [Simoes and Avouac, in prep.] that integrates crust incorporated into the wedge as well as the crust that participates to thickening. Also shown in the upper panel are the predicted uplift and erosion rates over the range (U and $-e$ respectively as derived from the equations of figure 4).

based on the stretching factor of 1.5 documented by [Lin, *et al.*, 2003]. The base of the upper crust of the undeformed continental margin has been set to 20 km [Shih, *et al.*, 1998]. A Moho depth of 30 km, that averages the ~28km for the southern transect and the ~33 km for the two northern ones [Kim, *et al.*, 2005; Shih, *et al.*, 1998; Yeh, *et al.*, 1998; Yen, *et al.*, 1998], has been considered. A Moho dip angle of ~11.5° for the downgoing plate beneath the orogenic prism is assumed, based on estimates from geophysical imaging [Kim, *et al.*, 2005; Lin, 2005; Shih, *et al.*, 1998; Yeh, *et al.*, 1998]. We assume that the lithosphere not incorporated into the orogenic prism subducts eastward below the Pacific plate. Lower crustal deformation at depth, below the range, could contribute to crustal thickening beneath Taiwan; however, such deeper processes are not modeled here. For numerical reasons, we only considered the thick insulating sedimentary cover in computing the initial conditions of our model. We did not distinguish the Cenozoic sediments and pre-tertiary basement since their thermal properties documented are shown to be similar (see compilation of parameters by [Song and Ma, 2002; Zhou, *et al.*, 2003], and the grid of densities by [Goffe, *et al.*, 2003]).

The geometry of the basal thrust fault was adjusted by error and trial; a thickness of 1km was attributed to this contact (figure 6). The model allows for underplating at the base of the range through the basal shear zone. The width and location of the underplating window as well as the incoming flux of material were also adjusted by error and trial. We considered different possible geometries of the contact between the orogenic wedge and the Pacific plate (figure 5). A 20 km thick oceanic crust [Yeh, *et al.*, 1998] was taken for the backstop of the range; the predicted surface heat flow matches what would be expected for a 48 Ma old [Seno and Maruyama, 1984] oceanic lithosphere (e.g. [Turcotte and Schubert, 2002]). The backstop was attributed the same horizontal velocity V_2 as the orogenic prism (figure 6). Eastern- and western-most boundary conditions were set so as to not allow for any lateral heat flow. Surface and bottom temperatures of 0 and 1350 °C were imposed; the “cold” surface conditions should not affect significantly the modeled low-temperature (U-Th)/He and fission-track ages on zircons.

The set of thermal and rheological parameters considered for the different domains are summarized in tables 1 and 2, and were fixed to usual values or to available constraints for the materials present in the region of Taiwan; radioactive production was considered uniform within the orogenic prism, although we might expect its rate to decrease with depth. A total shortening rate of 42 +/-2.5mm/yr has been considered for $V_1 - V_2$; however, we did not specify initially how the shortening is partitioned in terms of overthrusting and underthrusting (figure 5). In the case of the Himalaya of central Nepal, the spatial gradient of ^{40}Ar - ^{39}Ar ages on muscovite allowed for constraining V_2 because of the much broader scale of

the system and because of the high obliquity of the 350 °C isotherm to the particle trajectories and to the topographic surface [Avouac, 2003; Bollinger, *et al.*, 2004a]. A different line of reasoning is used here since these assumptions may not hold in Taiwan.

3.4 Initial conditions.

A simple juxtaposition without shortening ($V_1=V_2=0$) of the two plates, with the different domains described above taking into account an 8 km thick sedimentary layer [Lin, *et al.*, 2003] on the passive margin side, was considered as the initial condition of the model. Isotherms were relaxed until they reached a steady state. We did not try to model the initial oceanic subduction that most probably prevailed in the past over Taiwan as seen further south along the Manila Trench; data are rather scarce to test this earlier stage and tightly constrain it. In any case, given the total duration of our calculations (~ 10 Myr), the horizontal shortening V and the thermal diffusivity considered (table 1), the Peclet number characteristic of our models is $Pe \sim 560$, indicating that heat advection is much more efficient than conduction; the corresponding time diffusion over the whole lithosphere is of ~ 0.5 Ma so that any eventual thermal record of the initial phase of oceanic subduction would be rapidly obliterated. This is consistent with observations that temperatures within the wedge, 4-5 Ma after the initial relaxed isotherms, would only evolve by less than 10°C.

4. Modeling results.

Our analysis considered N110E sections perpendicular to the backstop (LV) and to the overall structural direction in Taiwan. We compared our modeling results with data along the three transects of [Beysac, *et al.*, in prep.], as indicated in figure 1: the southern and central cross-island highways will be considered here as our southernmost and northernmost sections; and the southern termination of the HR along the Choushui river will be our central transect.

4.1 Modeling the metamorphic history of the pre-Tertiary basement.

In our model, the metamorphic history of the TC depends essentially on the deep underplating window near the backstop. This portion of the Taiwanese range seems to have been the most long-lived structural feature so that its evolution would probably document most precisely how the total convergence is partitioned between V_1 and V_2 . We find that negative values of V_2 are needed to reach the observed surface peak temperatures. Indeed, in the case of a positive overthrusting velocity, particle paths of the TC cross the basal shear zone at shallower depths (figure 5) and would thus have undergone lower metamorphic conditions. Even with a negative overthrusting velocity, underplating would occur at maximum depths of ~ 30 km (figure 6) in order to exhume peak temperatures documented by RSCM data as high as ~ 500 °C (figure 2). These deep particle trajectories are actually needed because the high convergence rate does not allow for the orogenic wedge to get warm enough at lower depths; choosing a lower shortening rate of 39.5 mm/yr does not however change significantly these results. In any case a negative V_2 is actually consistent with the fact that the series within the western TC and eastern BR are inverted (figure 5). Moreover it indicates that the range has not been structurally growing and widening ($V_2 > 0$) but mostly rather eroding ($V_2 < 0$), even though the collision is very young; this is even true for the TC of the southern section that might represent a younger stage of the collision. An additional consequence of this finding is the implied east-dipping geometry for the contact between the pre-Tertiary basement and the LV, with a normal extensional sense of motion (figures 5 and 6). A value of ~ -2 mm/yr for V_2 (and thus $V_1 \sim 40$ mm/yr given the average convergence rate of 42 mm/yr) yields a very good fit to the surface gradient of thermo-chronometric data (above all (U-Th)/He ages on zircon) and to the spatial distribution of the peak temperatures (Figures 7 to 10).

Predicted thermo-chronometric ages are mostly sensitive to basal underplating rate; an underplating rate V_u of ~ 5.6 mm/yr and thus, by accounting for the vertical component of lateral advection $-V_2 \cdot \tan(\alpha)$, a total uplift rate of ~ 6.3 mm/yr over the TC (figure 6), does a very good job in matching the various data. The spatial distribution of reset ages appears to be mostly controlled by the westward extent of the underplating window; a ~ 40 km wide window, at the very back of the system, provides a very good fit to the thermo-chronometric data. On the other hand, we observed that narrowing the underplating window would increase the predicted inverted gradient in peak temperatures observed at the surface; a window of ~ 15 km width would account for the RSCM data. To solve for the inconsistency between the kinematics needed to fit low-temperature cooling ages, and the peak metamorphic temperatures on the other hand, we investigated the possibility of an underplating window that would have widened over time. We find actually that such scenario would reconcile both data sets if the underplating window width increased

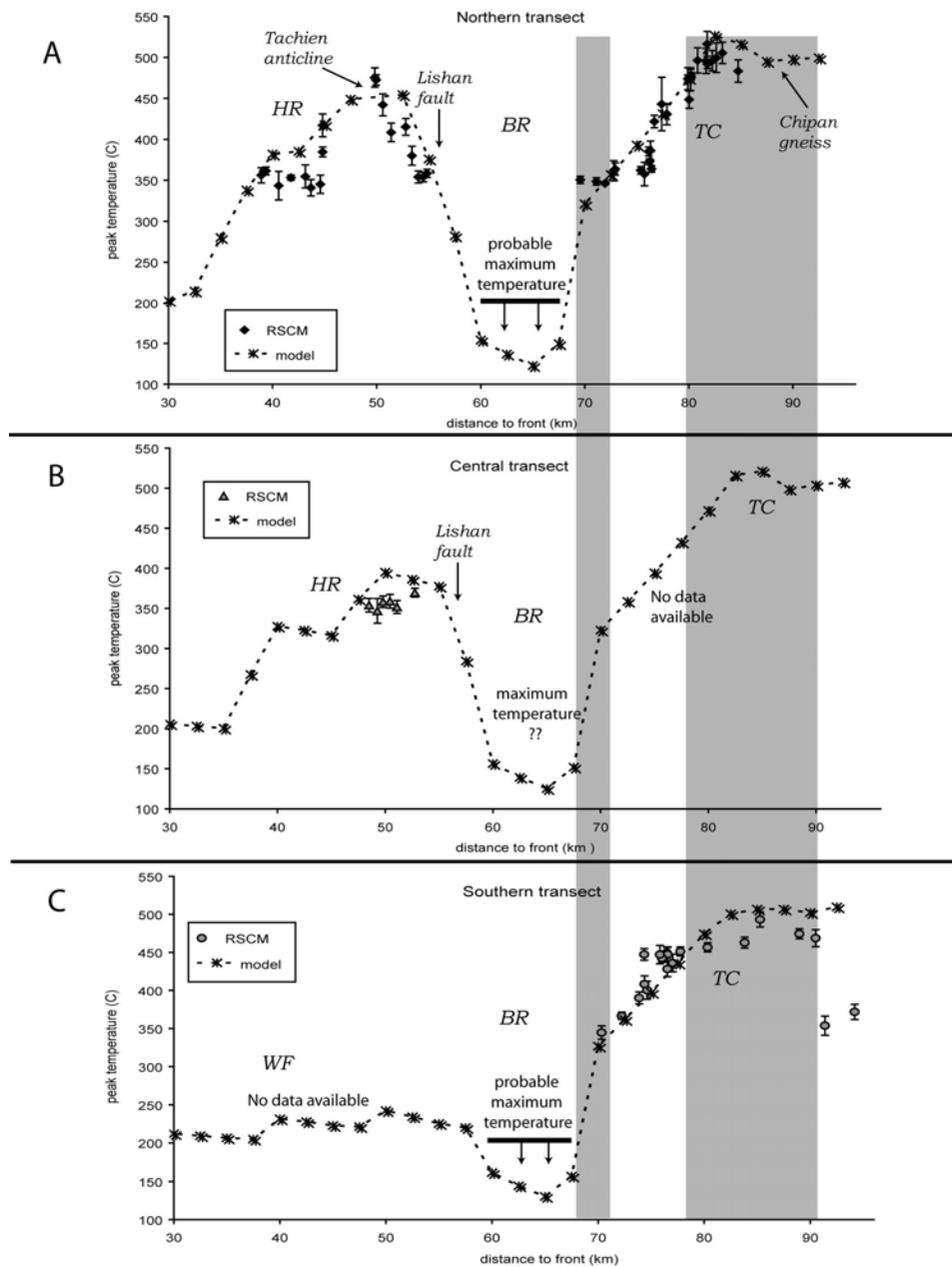


Figure 7: Peak metamorphic temperatures retrieved from the RSCM method [Beyssac, et al., in prep.] and predicted by our thermo-kinematic model for the northern (A), central (B) and southern (C) transects (figures 1 and 2). Observed temperatures below 330 °C within the BR were not reported since this value represents the lower limit of applicability of the method [Beyssac, et al., 2002]; alternatively a probable maximum temperature of ~ 200 °C may be inferred for this area based on the non-resetting of (U-Th)/He ages on detrital zircons [Beyssac, et al., in prep.]. Error bars represent a 2- σ interval. Peak temperatures over the range have been mostly acquired within the passive margin, except for the eastern limit of the BR and for the eastern portion of the TC that have been heated up during orogeny (shaded area). Overall, our model fits quite well the available peak temperatures, in terms of their values, their pattern and the observed gradients.

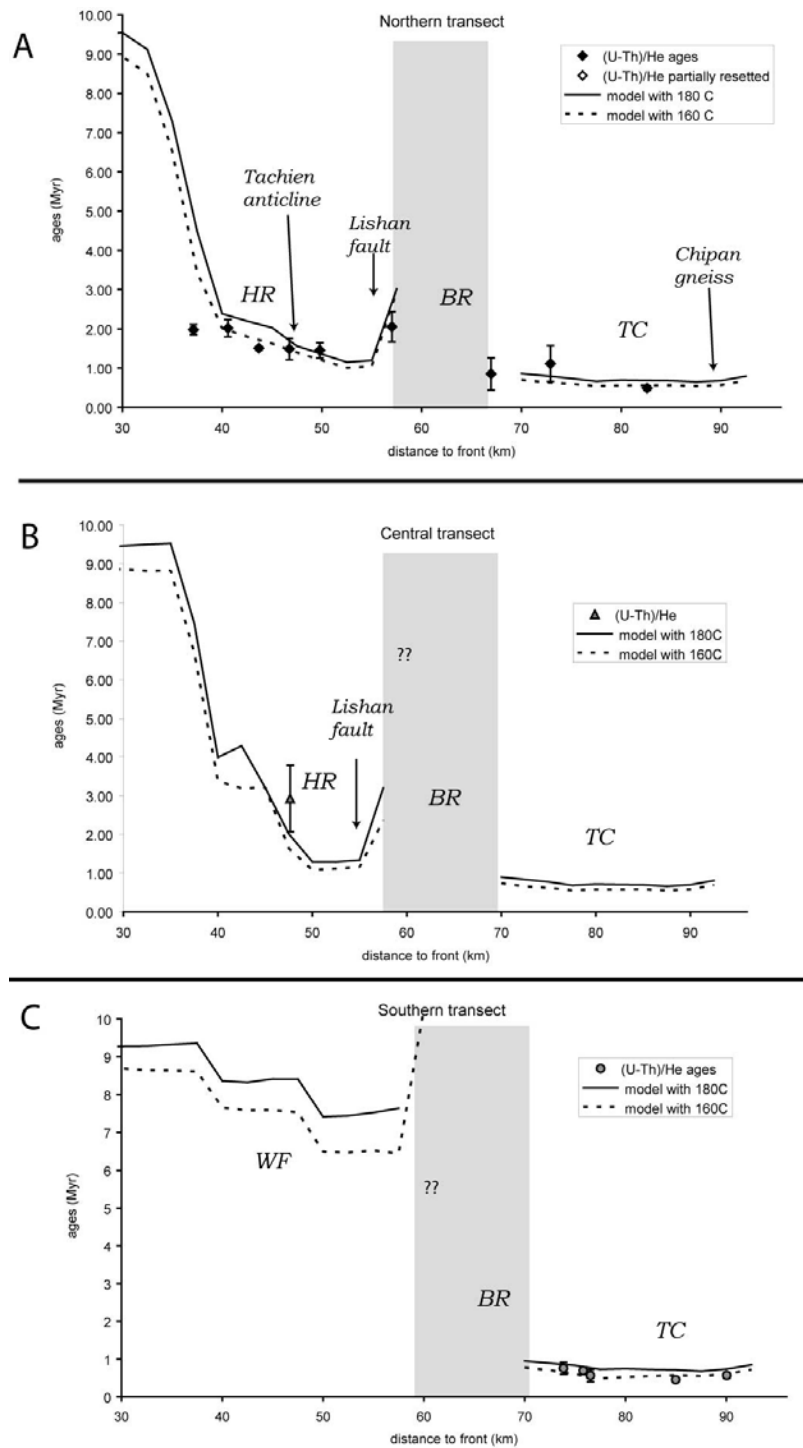


Figure 8: (U-Th)/He ages on detrital zircon [Beysac, et al., in prep.] with 2- σ error bars, and predictions from our thermo-kinematic model by assuming a closure temperature of 180 and 160 °C. Shaded area indicates where the ages are partially reset over the BR. The areas where no model predictions are reported indicate where the model predicts non-reset ages.

from ~10 km to ~36 km by 1.5 Ma ago. However, different tests show that the initial stage for the TC evolution may not be kept for a too long period of time, so as not to advect westward the high gradient of peak temperatures. Indeed this gradient appears to be mostly inherited from the thermal conditions in the passive margin, while the easternmost hottest temperatures are acquired during underthrusting of the Eurasian plate (figure 7). Ideally, the initial narrow window needs to keep running for ~9 Ma, and thus ~ 4 to 5 Ma after the thermal structure approaches some steady state. In any case, an increase in the overall eroded flux 1.5 Ma ago is consistent with the sharp increase in sediment supply within the LV basin documented by [Dorsey and Lundberg, 1988] between 1 and 2 Ma.

We checked for an eventual north-south temporal evolution of the TC. A 31 +/- 10/5 mm/yr northward aging of the collision would yield a time difference of 2.9 to 4.6 Ma between the two transects. In any case, we were not able to maintain the gradient of peak temperatures over this time by keeping a wide underplating window, or even by introducing other temporal changes in the incoming fluxes. The thermo-kinematic evolution of the TC would thus have been consistent and synchronous from north to south, as suggested by [Beysac, *et al.*, in prep.]. However, these results also indicate that the high gradient of peak metamorphic temperatures, as well as its location within the range, is a transient rather than a stationary long-lived feature.

4.2 Modeling the growth of the Hsueshan Range.

To model the thermal structure of the HR, we take into account the 31 +/- 10/5 mm/yr of southward propagation of maturation of this domain as deduced from the migration of sedimentary depot-centers [Simoes and Avouac, in prep.]. The three transects across the range documented by [Beysac, *et al.*, in prep.] illustrate the lateral evolution of the HR (figures 1 to 3). The structural architecture of the HR is modeled by allowing for continuous underplating across the shear zone. The minor exhumation observed over the BR (figures 2 and 3) requires that the underplating window modeled beneath the TC does not extend further west beneath this domain. This means in our model that the shear zone below the BR should parallel the Moho (figure 4). Given these different geometrical constraints on the detachment below TC and BR, we find that the underplating window beneath HR should lie at depths of ~ 10 to ~ 18 km (figure 6). A width of ~ 15 km for such window, as well as an uplift rate of ~ 4.25 mm/yr obtained with a 17 ° east dipping ramp, yields a good fit to the peak metamorphic temperatures and cooling ages, as well as their gradients (figures 8 to 11). In addition to that, the lateral evolution of the HR documented

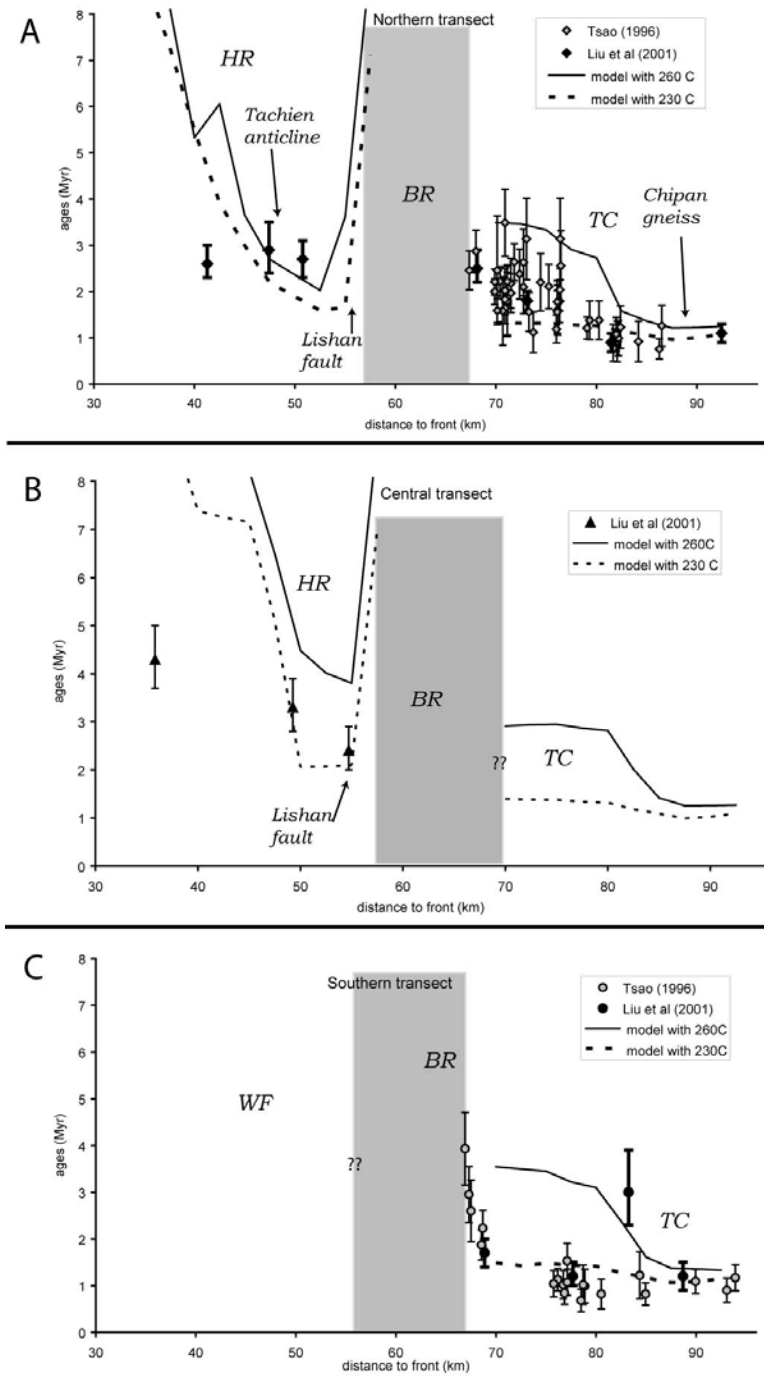


Figure 9: Fission-track (FT) ages on zircon from [Liu, et al., 2001; Tsao, 1996] with 2- σ error bars, and predictions from our thermo-kinematic model by assuming a closure temperature of 260 and 230 °C. Central ages were taken for the data from [Tsao, 1996]; in the case of the data from [Liu, et al., 2001], χ_2 ages were considered. Shaded area indicates where the ages are partially reset over the BR. The areas where no model predictions are reported indicate where the model predicts non-reset ages.

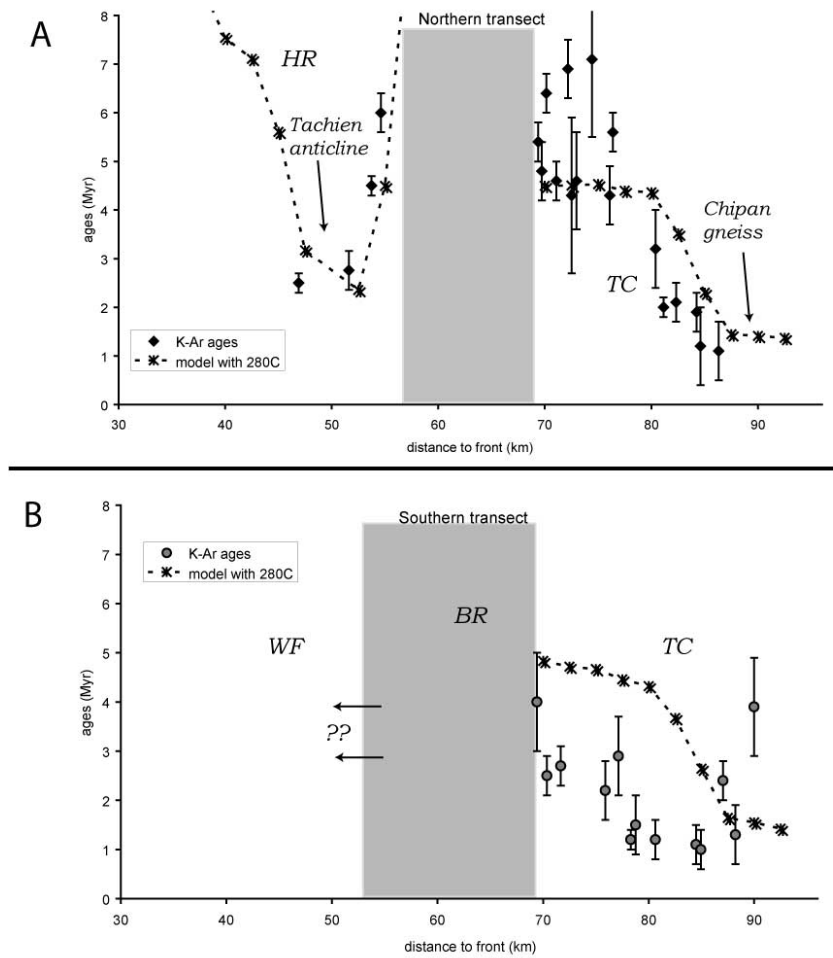


Figure 10: K-Ar ages on white micas fine fractions from [Tsao, 1996] with 2- σ error bars, and predictions from our thermo-kinematic model by assuming a closure temperature of 280 °C. Shaded areas locate non-resetted ages.

along the three transects is reproduced given the 31 mm/yr southward propagation rate (figures 7 to 10), provided that underplating initiated ~ 0.5 Ma before the stage equivalent to the southernmost section, at the latitude of the Chishui river south of Chiayi (figure 11). Complex duplexing within the eastern portion of the WF in this area is actually proposed by balanced cross-sections (e.g. [Hickman, *et al.*, 2002; Hung, *et al.*, 1999]), while the WF die out further south (figures 1 and 11). Such temporal and kinematic (figures 6 and 11) scenario accounts adequately for the pattern of peak metamorphic temperatures observed on all three transects along the HR or at an equivalent structural location (figure 7); the almost constant temperatures of ~ 360 °C west of this anticline were not accurately reproduced. In addition to that, the model predicts that these temperatures have been acquired within the margin, which is consistent with the proposed passive metamorphism of the HR [Beyssac, *et al.*, in prep.]; this predicted age of peak

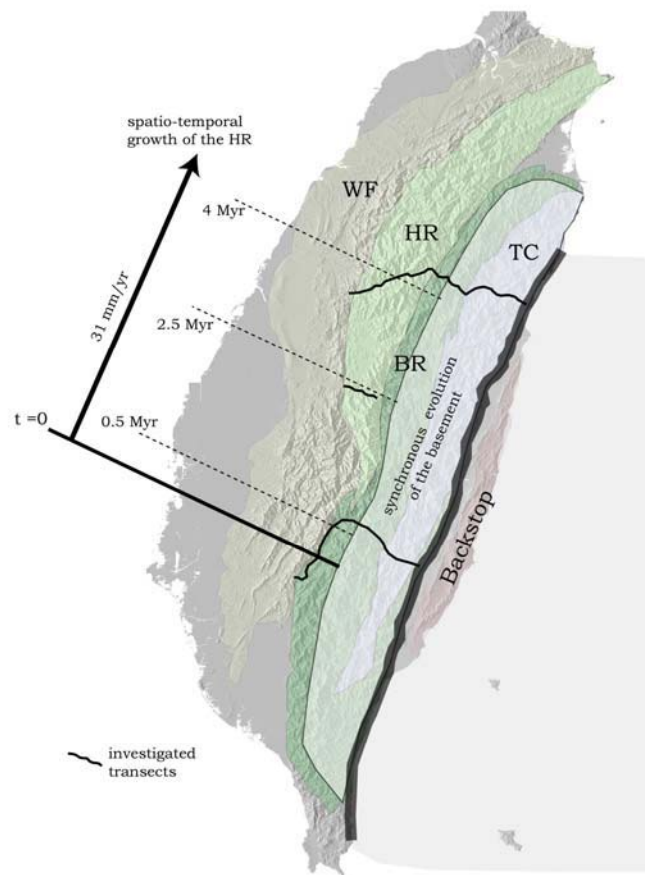


Figure 11: Modeled temporal evolution of the Taiwanese Range. Despite the southward propagation of the collision, a synchronous history for TC and eastern BR was able to account for the observed metamorphic and cooling evolution of these domains. On the other hand, the HR and its exhumation could be retrieved by assuming a northward growth of this structure of 31 mm/yr, based on the rate documented from the spatio-temporal evolution of the foreland basin [Simoes and Avouac, in prep.]. We actually found a very good fit to the available data (figures 7 to 10) by initiating HR slightly south of our southern transect; the timing allowed for each temporal stage in the growth of this unit is shown.

temperatures is dependent on the assumed initial conditions. It also provides a very good fit to the (U-Th)/He ages on zircon to the north (figure 8); however, the only data point along the Choushui transect may not allow for testing the modeled decrease over time in the gradient of this low-temperature ages between the two northern transects (figure 8). A good fit to the FT ages on zircon [Liu, *et al.*, 2001] could not be obtained, although the modeled ages are in the correct range of values (figure 9); this was not considered key since the accuracy of the data and the precise location of sampling is questionable (e.g. [Beysac, *et al.*, in prep.]). Finally, particle trajectories predict that the 4 Ma old underplating window beneath the HR to the north (figure 11) has been active for almost long enough to exhume the underplated

thrust sheets (figure 12). Indeed, according to the model, the rocks observed at the surface presently would have just been passively transported and uplifted above the underplated thrust sheets (figure 12), which would be consistent with the absence of non-coaxial deformation [Clark, *et al.*, 1993; Tillman and Byrne, 1995], and the normal series within the HR (figure 5). Adding 0.5 Ma of underplating below HR would have brought to the surface rocks that had gone through the window, but this would have degraded the fit to the observations. Continuous underplating beneath the HR appears thus to provide a very good approximation to the discrete stacking of thrust sheets, as in the case of the Lesser Himalaya [Bollinger, *et al.*, 2004a; Bollinger, *et al.*, *subm.*], although structures are not as long-lived in Taiwan.

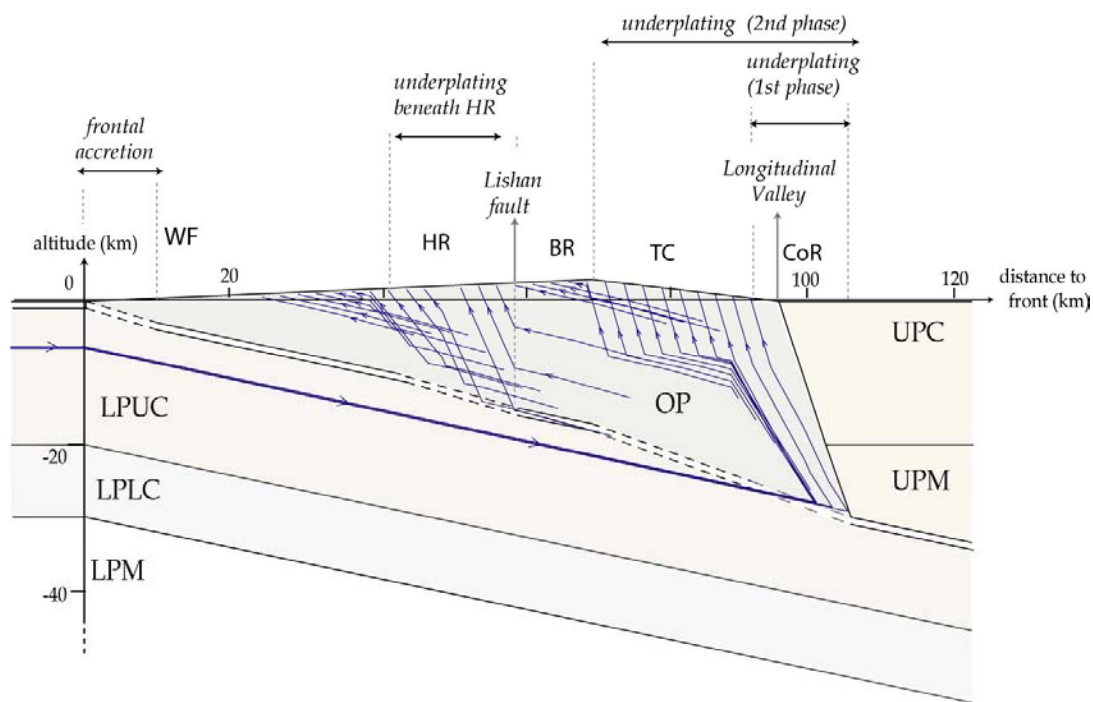


Figure 12: Geometry of the model and particle trajectories along which predictions of figures 7 to 10 have been computed in the case of the northern transect.

4.3 Final results for the southern, central and northern transects.

We combined the previous findings for the TC and HR to retrieve the thermal structure of the Taiwanese range along the three investigated transects (figure 13). The geometry of the shear zone retrieved to fit the constraints available for the TC, BR and HR was extended up to the front of the range (figure 6). To maintain a consistent velocity field, the basal contact was set parallel to the Moho geometry westward of

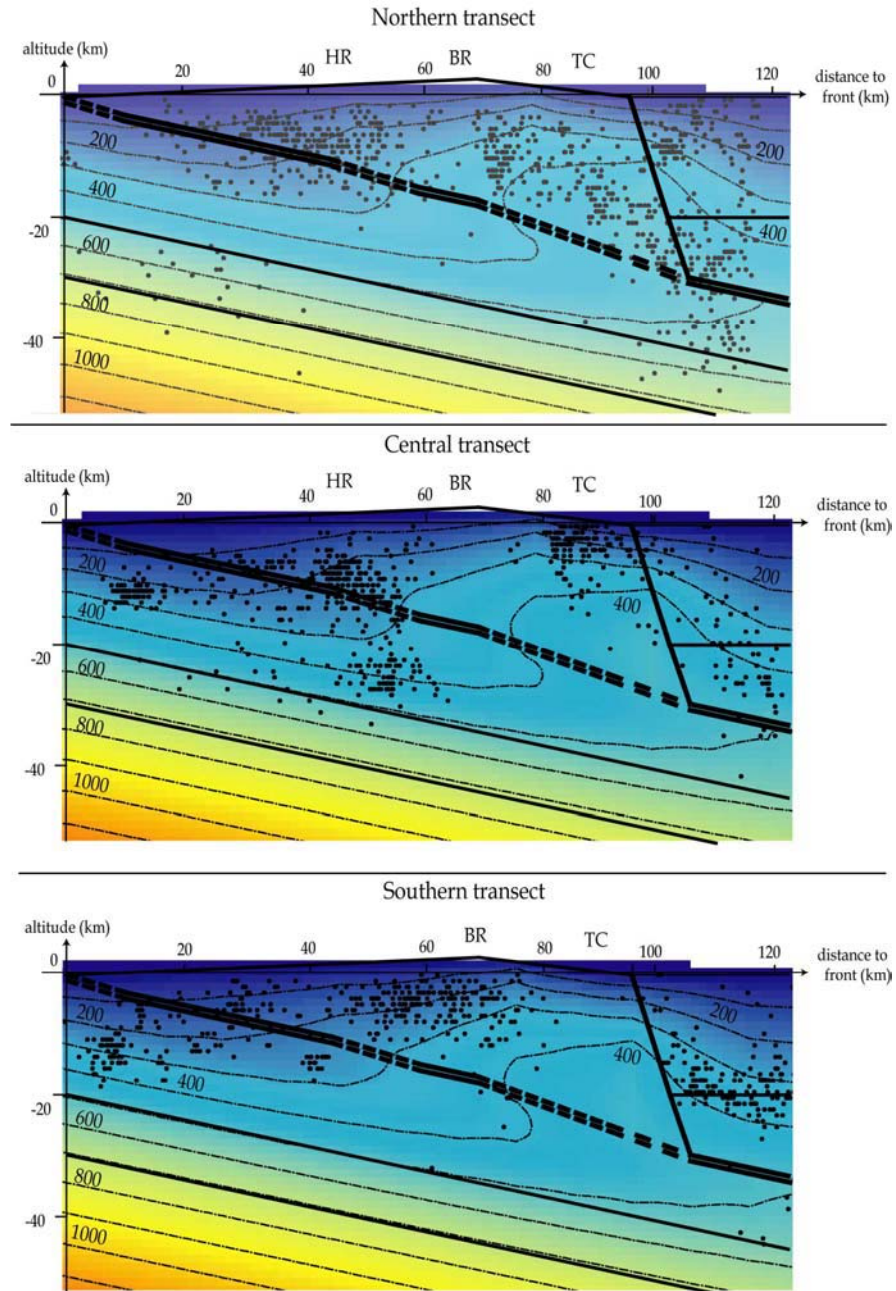


Figure 13: Derived final thermal structures for the three transects investigated in this study. Temperatures do not change significantly from the central to the northern sections, while they increase by $\sim 30\text{ }^{\circ}\text{C}$ at most within the prism from the southern to the central transects. This is most probably due to the very young underplating window to the south (figure 11), while further north this more long-lived feature would allow the thermal structure to approach some stationarity. Isotherms are represented every $100\text{ }^{\circ}\text{C}$ contour. Also represented is the seismicity from the CWB (Central Weather Bureau) catalog, retrieved along a 30km swath around each one of the three transects; only earthquakes of magnitudes over 3.5, from 1991 to 2000, have been plotted. No particular structure may be derived from this seismicity to support our derived deep geometry of the Taiwanese range. Interestingly, the seismic gap within the CR coincides quite well with the high topography, mostly for the northern and central transects, as well as the 350 to $400\text{ }^{\circ}\text{C}$ isotherms; this latter observation is also valid over the easternmost boundary of the prism.

the HR, with a ramp of $\sim 30^\circ\text{E}$ at most, if needed to reach the surface at the deformation front; “underplating” was allowed through this western ramp, and thus accounted for frontal accretion (figure 6), although the details of this process at the front are not investigated here. The TC has been modeled by a synchronous history from north to south, with widening of the underplating window 1.5 Ma ago; on the other hand, a continuous lateral growth of the HR, by accounting for a southward propagation of 31 mm/yr has been considered for this unit (figure 11). Figures 7 to 10 and figure 13 illustrate the fit to RSCM temperatures and to cooling ages, as well as the final thermal structures for the three transects; note that a good fit to K-Ar ages on white micas fine fractions [Tsao, 1996] could only be obtained by assuming a closure temperature of $\sim 280^\circ\text{C}$ at most, more realistic than the 350°C generally assumed [P. Renne, pers. comm., 2005]. We estimate the overthrusting and underthrusting rates V_2 and V_1 to -2 and 40 mm/yr respectively, implying a total shortening of ~ 42 mm/yr. Such scenario also ensures stratigraphic continuity between and within the Miocene BR and the Eocene to Oligocene HR units (figure 12). The Lishan lineament, in our model, mostly appears to be a zone of differential uplift between the HR and BR provinces, accommodated here by vertical shear (figures 6 and 12). The model does not account for the presence of rocks of BR affinity east of the TC to the south of Taiwan (figures 1 and 12); indeed, the predicted peak temperatures (figure 7) in our easternmost southern transect do not account for the decrease observed with RSCM data. Emplacement and evolution of TC may thus not be totally synchronous along strike, although these variations should only be minor.

Comparison of the three transects allows for verifying the validity of the 2D assumption (figure 13). Only a small temperature increase of $\sim 7^\circ\text{C}$ at most within the prism is observed between the northern and central sections. However, the thermal structures between the central and the southernmost transect appear to vary more significantly; indeed, temperatures increase by $\sim 30^\circ\text{C}$ at most within the whole wedge. The differences between these transects most probably arise from the differential growth of the HR, since the TC follows a synchronous scenario along strike. In fact, 0.5 Ma after underplating initiated below the HR, at the equivalent of the southern section, the thermal structure may not be already stationary; comparison of the different stages documented here indicate thus that steady state may be approached very rapidly, after ~ 3 to 4 Ma, in between the central and northern transects (figures 11 and 13). The 2D hypothesis may thus still hold for Taiwan, although mostly questionable further south, where the transition from subduction to collision is not modeled in this study. Finally, although the 2D-assumption may have been questioned because of the ubiquitous presence of left-lateral shear, the very good fit of our model to all

data indicates that this lateral transport may not contribute significantly to the thermal evolution of the Taiwanese range.

4.4 Predicted P-T-t paths.

The predicted temperature-time (T-t) for the Chipan gneiss within the northern TC (figure 1), and pressure-temperature-time (P-T-t) paths for particles from the TC, BR and the HR along the northernmost section are represented in figures 14 and 15. A very good fit is observed for the cooling history of the Chipan gneiss (figure 14), except for the low-temperature ages on apatites [Beyssac, *et al.*, in prep.; Willett, *et al.*, 2003]. However, the ^{40}Ar - ^{39}Ar age on biotite of 7.7 Ma [Lo and Onstott, 1995] fits well the initial conditions in the margin, but would not have been resetted by the subsequent heating of up to ~500 °C during orogeny as indicated by petrologic data and RSCM temperatures. The significance of this data is unclear as it could represent a cooling age or a crystallization age and it may be altered by late chloritization of the biotites [Lo and Onstott, 1995]. Interestingly, we were able to reproduce increasing temperatures along the particle path by ~ 7 Ma, very close to the 6.5 Ma age of initiation of the collision [Lin, *et al.*, 2003]. This timing is actually related to the duration allowed for the first phase of narrow underplating below TC, that had been tightly adjusted in the model to fit the gradient of RSCM peak temperatures; it seems thus that our model is able to satisfy several independent constraints on the metamorphic and temporal evolution of the range.

The clockwise P-T-t path within the TC indicates heating within the orogenic prism and subsequent rapid cooling. The maximum P-T conditions of ~500 °C and ~8 kbars (figure 15) are in good agreement with those estimated for the blue schists in the easternmost part of TC along the LV contact [Beyssac, *et al.*, in prep.; Ernst and Jahn, 1987; Liou, *et al.*, 1975], but might be surprising because of the poor mineralogy of the ubiquitous slates in the Yuli belt (eastern TC); however, the fast kinetics of burial and exhumation, eventual limited amount of constitutive fluids in minerals, the lack of index mineralogical assemblages at such P-T conditions and simply the initial chemistry of these rocks are reasonable explanations for the absence of a clearly expressed mineralogy expected for such maximum P-T conditions [Beyssac, *et al.*, in prep.]. P-T paths for the BR and HR reveal the general cooling and decompression of these rocks during the last orogeny, although initiation of underplating below the HR, 4 Ma before the northern transect, would have slightly heated up this domain (figure 15).

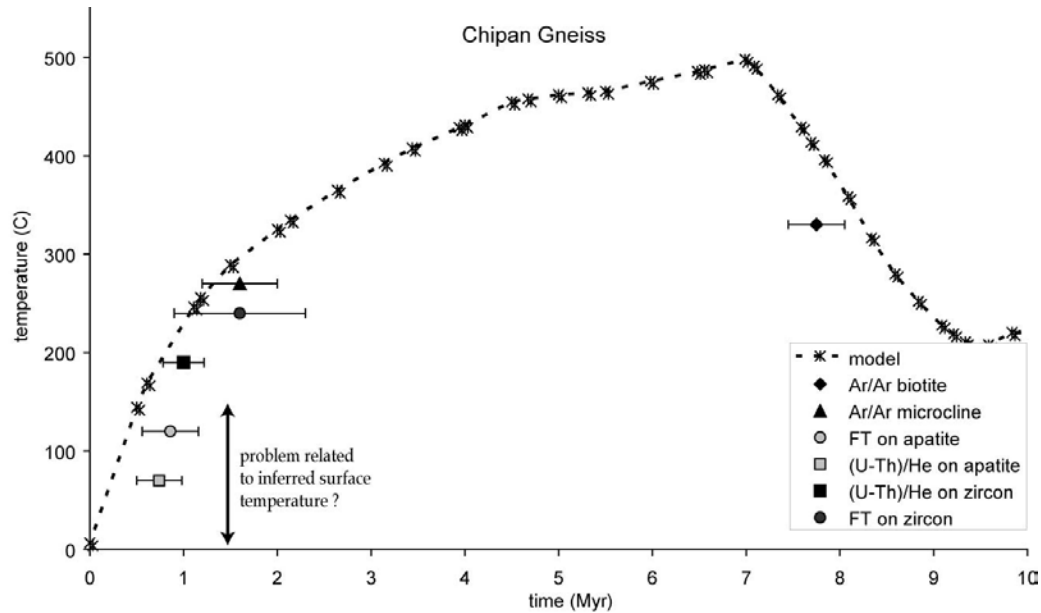


Figure 14: Time-temperature path predicted for the well-documented Chipan gneiss along the northern transect (figure 1). $^{40}\text{Ar}/^{39}\text{Ar}$ ages on biotite and microcline are from [Lo and Onstott, 1995]- FT (central) age on zircon from [Liu, et al., 2001] – (U-Th)/He ages from [Beyssac, et al., in prep.] and FT (central) age on apatite from [Willett, et al., 2003]. Error bars are taken to represent a $2\text{-}\sigma$ uncertainty on the ages; closure temperatures are those proposed in these different initial papers, and we did not account on this plot for any possible variability on these values. Overall, our model fits well the data, except maybe for the very low-temperature cooling history of the gneiss, most probably because this latter may be too sensitive to the model surface boundary conditions. Interestingly, the predictions also go close to the $^{40}\text{Ar}/^{39}\text{Ar}$ age on biotite of ~ 7.7 Myr [Lo and Onstott, 1995], although our model, as well as other constraints on the metamorphic history of the gneiss, would suggest that subsequent heating of the gneiss up to $\sim 450\text{-}500$ °C should have resetted this age; see text for more details. These different constraints have been taken over the Chipan massif, but not on the same samples.

4.5 Sensitivity tests

We tested here the sensitivity of the model to different parameters. The location and width of the underplating windows beneath HR and TC are well constrained by the spatial distribution of resetted cooling ages, as well as by the gradient of exhumed peak temperatures.

As for the kinematic parameters, a slight increase of V_2 by 0.5 mm/yr degrades the fit to the data. Indeed increasing V_2 induces a westward transport of the inverted thermal gradient, as well as of the pattern of resetted ages; but more importantly, the gradients of cooling ages become too gentle in light of the observations. A decrease in the overthrusting rate would imply ages slightly too old. We also tested the variations of V_1 by keeping V_2 to its best fitting value of -2 mm/yr, with account on the uncertainty on the shortening rate across the range as assessed by [Simoes and Avouac, in prep.]. A decrease in V_1 mostly affects cooling ages since the underplating flux directly depends on this rate; however, the thermal structure is not significantly affected by variations of V_1 within the possible range of values. These rates

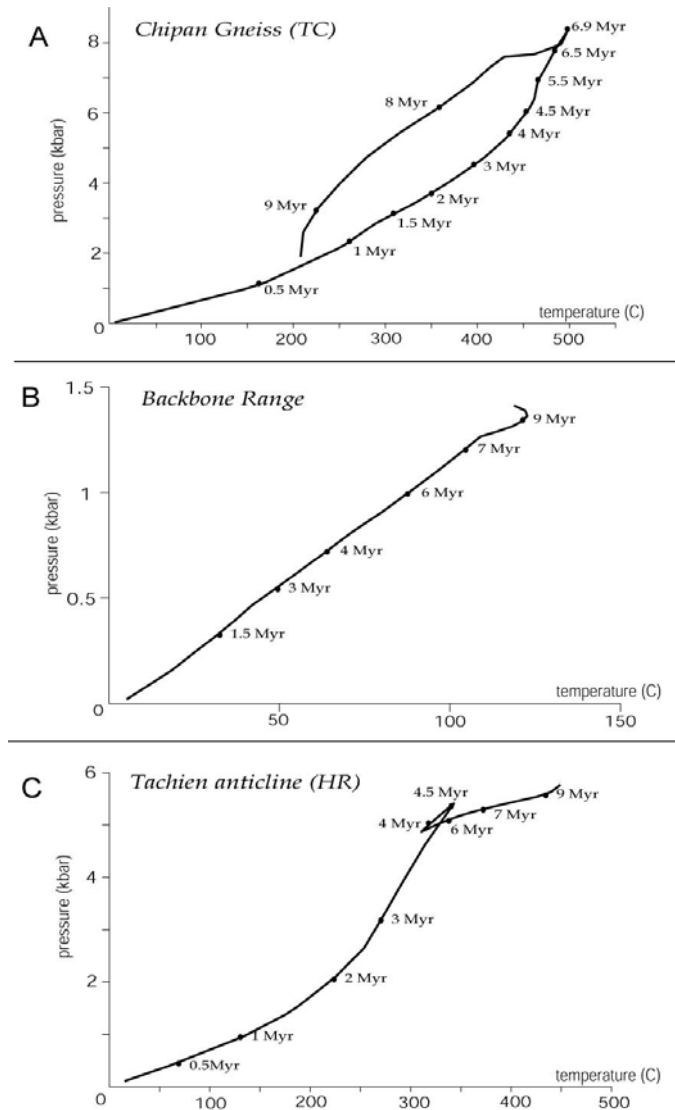


Figure 15: PT-t paths predicted along the northern transect, and more specifically for (A) the Chipan Gneiss to illustrate the modeled evolution of TC, (B) the BR, and (C) the heart of the Tachien anticline as for the deepest exhumed portion of the HR (figure 1). Only the easternmost range, within the TC, has been significantly heated during the Taiwan orogeny, while the BR and HR have cooled down from their initial temperatures in the passive margin. By ~ 4 Myr, it appears however that the Tachien anticline was slightly heated up, most probably because of initiation of the underplating window beneath this domain (figure 11).

V1 and V2 are thus well constrained: ages are controlled by V1 through its impact on the basal incoming flux, whereas V2 mostly affects the gradients of cooling ages and temperatures.

The rate of north-south propagation of the evolution of the HR may affect the results, by changing the time lag between sections; we tested this by assuming the extreme rates of 41 and 26 mm/yr allowed from the analysis of [Simoes and Avouac, in prep.]. Indeed, peak metamorphic temperatures within the HR increase slightly by less than 10 °C for a slower southward propagation, but this case predicts in turn

temperatures too high, and (U-Th)/He ages too young for the Choushui transect; the opposite is observed for the highest lateral propagation rate. Overall, the kinematic parameters are quite tightly constrained by the diverse complementary datasets.

The thermal structure of the range is mostly affected by changes in thermal parameters such as heat produced by radiogenic decay of elements. We considered in our model a production rate of $1.7 \mu\text{W}/\text{m}^3$ based on the average value measured over the varying lithologies across the CR (see compilation of data from [Chang, 1989] by [Song and Ma, 2002] over the range) (table 1); a rate of $1 \mu\text{W}/\text{m}^3$ has been used by [Barr and Dahlen, 1989], while measurements of $2.45 \mu\text{W}/\text{m}^3$ have been performed in the basement in the Pearl River Mouth [Rao and Li, 1994]. Cooling ages and surface heat flow appear to be the most affected by such extreme radiogenic heat production rates, but differences are not significant. On the other hand, shear heating has a strong influence in the thermal structure as well as on the predicted peak temperatures and cooling ages. Temperatures higher by $\sim 20 \text{ }^\circ\text{C}$ may be retrieved within the HR by inferring a diabase rheology with a maximum shear stress of 100 MPa for the shear zone; in this case, predicted (U-Th)/He and fission track ages on zircon are too young, temperatures within the TC and heat flow over the HR too high in light of the available data.

The interplay between the different parameters and the numerous independent constraints on the thermo-kinematics of the range allow for tightly constraining our thermo-kinematic model on all three sections.

5. Discussion

5.1 Thermo-kinematics, deformation within the wedge and geometry of the structures at depth.

A normal fault between the CR and LV?

In the thermo-kinematic model proposed here, we find that the pattern of cooling ages and peak metamorphic temperatures, as well as the structural features of the Taiwanese range may be well-fitted by assuming a negative overthrusting velocity V_2 (figure 6). This is in contrast with the general view of doubly vergent orogens (e.g. [Koons, 1990; Willett, et al., 1993]), where underplating and underthrusting rates would be high relatively to the basal shear zone so as to account for the growth of the orogenic prism (figure 5). Our study shows in fact that such kinematics may not hold in Taiwan. The erosive mode

proposed (figure 5), similar to the Himalayan case [Bollinger, *et al.*, 2004a; Bollinger, *et al.*, *subm.*], would suggest that the structures are relatively long-lived and mature, although the collision is quite young; this is most probably the case since high deformation and erosion rates would allow for reaching rapidly some orogenic steady state`.

As pictured in figure 5, a negative overthrusting velocity in turn implies an east dipping extensional contact between the orogenic prism and its backstop. The nature of this major contact, along the LV has been controversial and is still a matter of debate. Indeed earlier cross-sections over Taiwan, based on the critical wedge theory and the topographic slope (e.g. [Davis, *et al.*, 1983]) have proposed that a west dipping thrust fault would mark the contact between the CR and the LV; [Carena, *et al.*, 2002] also suggested that the pattern of background microseismicity may be compatible with such geometry. However, the steep rise in topography from the low elevation LV to the ~3000 m high peaks in eastern CR, with observable morphological triangular facets, would rather favor a normal contact; also some structural, petrologic and seismic observations do not corroborate the backthrust scenario. Indeed, brittle to ductile extensional shear zones, observed within the easternmost CR of Taiwan [Crespi, *et al.*, 1996], would support a normal contact with the backstop; exhumation of the blueschists present within the Yuli belt, eastern TC [Beysac, *et al.*, *in prep.*; Ernst and Jahn, 1987; Liou, *et al.*, 1975], would also be facilitated by such corner-flow type of kinematics. Focal mechanisms below this internal part of the CR prove to be extensional rather than compressional down to depths of ~ 15-20 km [Kuoehen, *et al.*, 2004], on east dipping oriented planes; more particularly, in central Taiwan, a major east dipping normal contact down to these depths has been mostly illuminated by background seismicity after the ChiChi earthquake [Gourley, *et al.*, 2004]. This is also consistent with the synorogenic extension derived from GPS data, interpreted to favor exhumation of a crustal slice beneath the CR [Bos, *et al.*, 2003]. However, stresses and proposed geometries of the contacts may vary with depth; compression indeed is seen in focal mechanisms of earthquakes to deeper depths of ~ 30 km, but could be associated with the LV thrust fault beneath the CoR [Kuoehen, *et al.*, 2004]. This suture contact may thus be particularly complex. Finally, our thermo-kinematic modeling of the Taiwanese range brings additional insights into this debate, since the geometry of the contact with the backstop was not initially assumed, but rather adjusted to fit the available thermal constraints; a contact with a normal sense of motion is rather needed to fit the available constraints on the long-term evolution of the range (figure 5 and section 4.1).

The retrieved geometry of this easternmost boundary of the prism also implies that the underplating window would extend eastward to about the coastline of Taiwan (figure 6), so that some uplift may be

transmitted to the upper plate, below the CoR. In addition to that, although deep crustal deformation and thickening was not accounted for in our thermo-kinematic modeling, our best-fitting corner-wedge geometry to the east implies that crustal thickness is at its most not beneath the CR but indeed below this emerged portion of the Philippine Sea Plate (figure 6). This is indeed consistent with the Moho imaged by wide-angle offshore and onshore seismic experiments of [Shih, *et al.*, 1998; Yeh, *et al.*, 1998], but contrasts with the geometry proposed by [Kim, *et al.*, 2005] based on the sole 7.5 km/s velocity contour that is deeper beneath the CR than the CoR. In any case, uplift related to the deeper underplating window and greater crustal thickness would most probably contribute to the emersion and gentle topography of the CoR. Further geophysical investigations may be necessary to document precisely the structures at depth, eventual thickening of the lower crust and the nature of the major contacts in eastern Taiwan.

Background seismicity, thermal structure and geometry of the basal shear zone.

Geophysical constraints on the deep structures beneath the CR are rather scarce to test our proposed geometry; however background seismicity may still provide some insights. Earthquakes of magnitudes over 3.5 (Central Weather Bureau catalog), from 1991 to 2000, were plotted on figure 13, along with our modeled geometry and thermal structures. Interestingly, the northern and central transects show a similar pattern, with a cloud of seismicity beneath the HR, a seismic gap further east beneath the BR and an overall east dipping cloud (mostly pronounced to the north) in the TC and CoR area; to the south, the gap shifts eastward below the TC, and seismicity is more rare. Overall, extinction occurs over the areas of highest altitudes, within the BR, which might suggest that topography controls background seismicity, most probably by influencing the general stress field. Indeed, the major change from NW-SE compression in western Taiwan to extensional strain within the eastern CR as documented by GPS data [Bos, *et al.*, 2003] occurs over the BR; a similar topographic control has been actually observed and modeled in the Himalayas of central Nepal [Bollinger, *et al.*, 2004b]. However, we may not rule out a thermal control on the seismicity since this extinction also coincides with the $\sim 300\text{-}400$ °C isotherms (figure 13); this control is remarkable to the east of the HR, but also mostly below the TC and CoR, over the southern and central transects. However beneath the TC in the northern section, the pattern of seismicity does not obey any of these different rules, most probably because of the complex deformation occurring at the plate boundary. Investigating focal mechanisms as well as the stress field should help better understand these observations. In any case, the pointed correlations between seismicity and our derived thermal structures support the model proposed in this study.

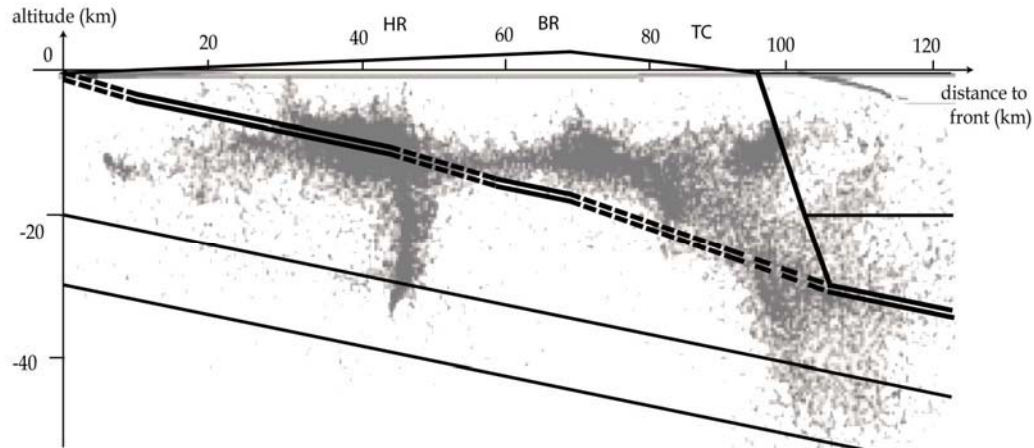


Figure 16: Comparison between the geometry of the orogenic wedge adjusted in our model, and relocalized micro-seismicity by [Carena, et al., 2002]. Although our basal shear zone does not fit their proposed detachment and backthrust beneath Taiwan, their seismicity is compatible with our proposed structures at depth.

These seismicity data however do not provide much information on the deep structures, although they are compatible with the location of the underplating window beneath HR, as well as with the easternmost contact between the wedge and backstop (figure 13). Earthquakes of smaller magnitudes over a similar time period have been relocalized and collapsed onto an eventual common decollement by [Carena, et al., 2002]; the results actually showed that background micro-seismicity would be compatible with a detachment running over the entire Taiwanese range (figure 16). Although our best-fitting geometry is different from the geometry of the decollement proposed by [Carena, et al., 2002], which is running between 10 to 15 km depth over most of the range and then stepping up to the surface as a backthrust along the LV, it is still compatible with their overall relocated clusters of seismicity (figure 16); except for the steep tear fault illuminated beneath the HR and the diffuse cluster at the far eastern bottom of the modeled orogenic prism, all background seismicity is indeed within the wedge, mostly on, or right above, our modeled main basal contact (figure 16). The geometry proposed by [Carena, et al., 2002], in its details, would most probably not have been capable of accounting for the metamorphic evolution of Taiwan; indeed, a backthrust splaying from the main detachment at ~ 15 km depth is geometrically not compatible with the long term evolution of the range, and would most probably not have exhumed peak temperatures as high as those documented by RSCM. Finally, the detachment proposed by [Carena, et al., 2002] is based on their interpretation of seismicity observed over about a decade in central Taiwan, at the latitude of Taichung; our model, on the other hand, is meant to reproduce the longer term spatio-temporal evolution of the whole CR.

In addition, in both seismicity plots (figures 13 and 16), it seems that clusters are concentrated in the vicinity of the underplating windows, beneath HR mostly but also TC for the northern and central transects. Indeed, deformation may be concentrated where thrust sheets are being stacked at the base of the orogen. Also, beneath BR, where topography is at its highest, and where the $\sim 350^{\circ}$ C isotherm is first crossed going eastwards along the basal shear zone, seismicity becomes extinct and no major rock uplift takes place. This in turn questions the factors controlling the localization of underplating windows, and its relation to seismicity and thermal structure.

Finally, it should be noticed that it would be possible to modify the geometry of the basal detachment in our model to fit better the seismicity pattern. In this case, we would need to modify the Moho geometry accordingly, because in our model the amount of underplating is controlled by the difference in the dip angles between the Moho and the basal shear zone.

5.2 Incoming and outgoing fluxes, and implications on orogenic growth.

Predicted average erosion rates over the Taiwanese Range.

Predicted erosion rates for the last 1.5 Ma range from ~ 0.4 mm/yr in the BR to ~ 6.1 mm/yr in the TC (figure 6), and yield an average value of ~ 3.21 mm/yr over the whole width of the range. This is close to the 3.9 mm/yr average erosion rate derived by [Dadson, *et al.*, 2003] based on 30 yr of measurements of the sediment suspended load in major Taiwanese rivers, although these measurements do not incorporate bedload and do not account for a comparable time scale. Previously proposed long-term erosion rates of ~ 3 to 8 mm/yr on average were based on cooling ages in the more internal portions of the range only, assuming a 1-D 30° C/km surface thermal gradient [Willett, *et al.*, 2003]. Our model used the same datasets on FT ages, but complemented with recent additional thermo-chronological results [Beyssac, *et al.*, in prep.]; in addition to that, we account for the overall temporal evolution of the range and 2D thermal structure of Taiwan with lateral advection of heat. We believe thus that our results are more reliable; also they allow for assessing not only the erosion on the more internal parts of Taiwan, but also the average value over the whole range, essential to quantify fluxes of material involved in orogenic growth.

This rate is essentially valid over the last 1.5 Ma after major rearrangements lead to increasing underplating beneath the TC; during the first phase, the average erosion rate was slightly lower (~ 3.1 mm/yr). Indeed, since the basal shear zone geometry is tied to its deepest point beneath the TC to fit

the high peak temperatures, and to the front of the range, a decrease in the incoming flux within the TC would actually be geometrically compensated by an increase of the incoming flux further to the front; also the stable topographic contribution to the erosion rate is negligible in light of these average uplift rates (figure 6).

Temporal evolution in the mode of orogenic growth.

From the width of each underplating window and from the angle between the thrust and Moho (figure 4), the thickness h' of the slice of crust incorporated into the range is constrained to an average of ~ 7 km. This is true for any different phase modeled in our study, that is with or without emplacement of the HR, and during the narrow or wide underplating window beneath the TC. Indeed, the geometry of the Moho and the overall geometry of the shear zone do not vary with time in the model. What changes between the two stages is the relative contribution of frontal accretion, and underplating beneath HR and TC, to this total 7 km of incoming crust. Indeed, during the initial phase for the TC, ~ 80 % of this incoming flux is accommodated further west, by underplating beneath HR (≤ 18 to 19 % of the total if this structure is already growing), and mostly by frontal accretion. The increase in the incoming flux below TC over the last 1.5 Myr reverted this partitioning: ~ 70 % the incoming flux is then taken up below the eastern CR, while contribution of the westernmost structures decreases to ~ 30 %, with still 18 to 19 % on HR. The predicted contribution of frontal accretion to the growth of the range seems thus to have decreased over time, since it accounted for 80 % of the initial incoming flux at the earlier stages, and has only accounted for ~ 10 % of this flux over the last 1.5 Ma; alternatively, the contribution to mountain-building of underplating below the more internal portions of the orogen has increased over time. Whether this is a typical evolution from an accretionary wedge, as further south along the Manila Trench, to a mature collisional orogen as in central Taiwan is an interesting issue that would need further investigations.

What controls this evolution in the mode and distribution of orogenic growth in Taiwan may indeed be questioned. Increasing deformation and rising temperatures within the growing and maturing wedge may play a role. Such scenario would imply a laterally varying timing of these major changes, which actually holds for emplacement of the HR. However, the major change is related to the widening of the underplating window beneath TC, which occurred synchronously ~ 1.5 Ma ago over the whole range. Such large spatial extent of the phenomenon may suggest it is rather climatically controlled. Indeed, 1.5 Ma coincides with initiation of the Pleistocene, known for the dramatic changes in climate with glacial and interglacial times (e.g. [Shackleton, *et al.*, 1988]). On the other hand, this 1.5 Ma timing also coincides

with the indentation of the Peikang High to the orogen at the latitude of the Puli Basin [Simoes and Avouac, in prep.]. The complex geometry of the underthrusting passive margin (e.g. [Teng, 1990]) may have also played a major role in these re-arrangements. Indeed, modeled particle trajectories (figure 12) suggest that the rocks now within the TC have been dragged deeper than those now in the HR or BR; however the initial positions of the particles now in the TC were in the passive margin at depths shallower than the initial positions of particles now in the HR and BR. The pre-Tertiary basement complex may thus have been related to a horst structure while the metasediments were deposited within deeper grabens, as already proposed to interpret the different depositional facies in HR and BR [Clark, et al., 1993; Lee, et al., 1997; Tillman and Byrne, 1995]. The decoupled temporal evolution between the western and eastern CR may thus also be linked to these differences in initial conditions.

Incoming/outcoming fluxes and implications on crustal deformation.

The average erosion rate of ~ 3.2 mm/yr and the thickness h' of incoming crust of ~ 7 km predicted by our thermo-kinematic model may be compared to the kinematics derived by [Simoes and Avouac, in prep.]. They found that a thickness h of ~ 8.4 to 8.6 km of crust needs to be incorporated to the orogen to balance the 3.2 mm/yr of erosion. The slight discrepancy between these two estimates may derive from the two different assumptions behind h and h' . Indeed, the analysis of [Simoes and Avouac, in prep.] does not only integrate the growth of the sole orogenic prism: their variation of A , the cross-sectional area of their wedge, as seen from the changes in lateral width of the range, includes also in fact observed crustal thickening through their chosen taper angle. In the present study, on the other hand, we did not account for deep processes, but focused only on the growth of the orogenic prism. It might consequently be suggested that the ~ 1.5 km difference between h and h' would eventually contribute to crustal thickening beneath the Taiwanese range. The remaining 21.5 km of crust ($H - h$, with H as in figure 6) would then be lost by subduction beneath the Philippine Sea Plate; as further discussed by [Simoes and Avouac, in prep.] and below in the next section, this scenario may be realistic although the continental slab has not been imaged by geophysical imagery. Our study, coupled with the kinematic assessments of [Simoes and Avouac, in prep.], provides thus quantitative insights into the different fluxes of material participating to orogenic processes in Taiwan.

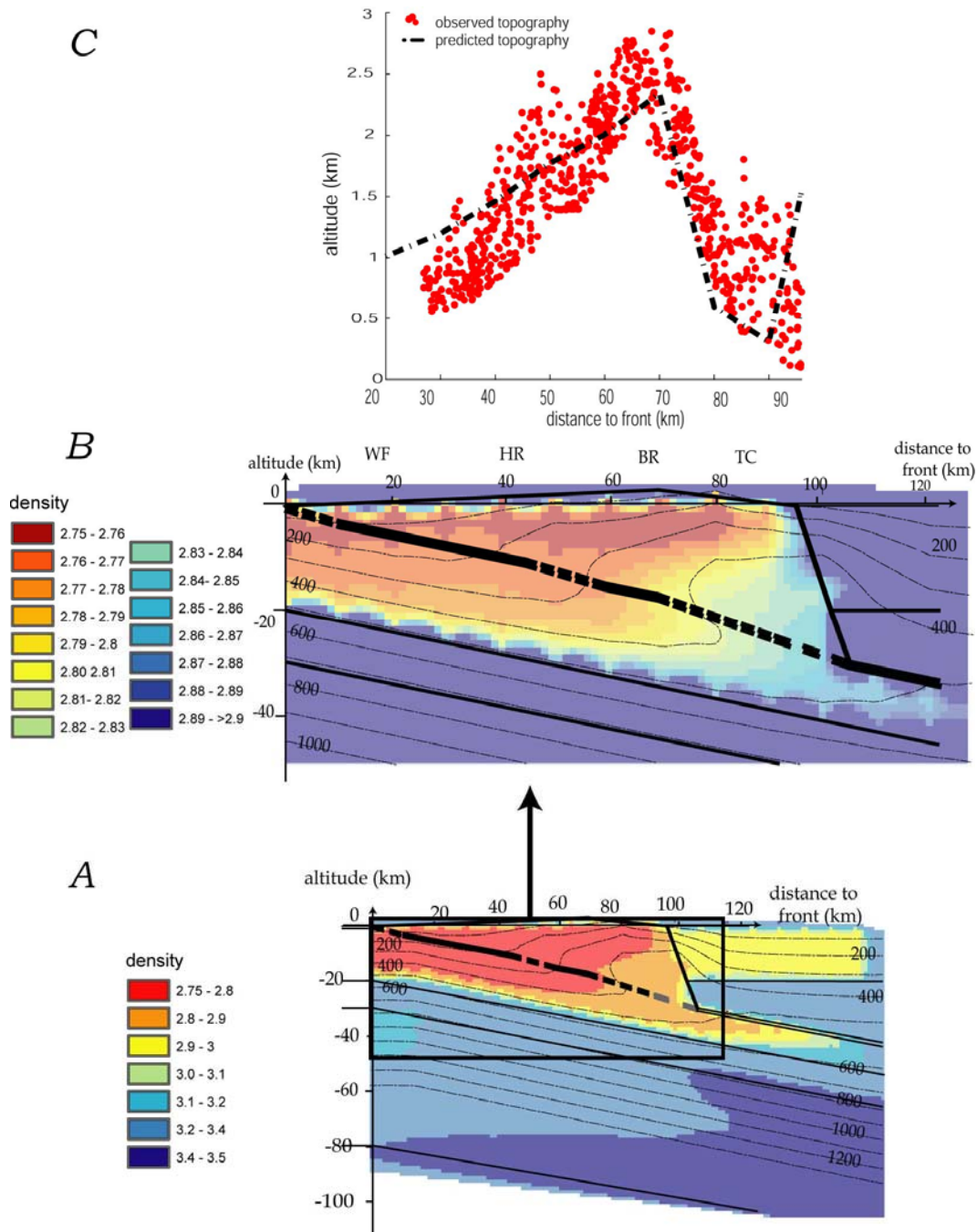


Figure 17: Predicted densities and topography in the case of the northern transect. See text for further details and discussions.

(A) Densities predicted from the compositions detailed in table 1 in the case of the PT conditions computed in our model, using the procedures described in [Bousquet, et al., 1997]. Inset locates (B). Fine lines indicate the isotherms of the temperature field shown in figure 13.

(B) Details within the orogenic wedge of the densities shown in A.

(C) Topography predicted from the distribution of densities shown in A by assuming local isostasy and compensation within the asthenosphere (procedures described in [Henry, et al., 1997]). The observed topography (red dots) is taken within a 20 km wide swath across the northern transect.

5.3 Metamorphic transformations, subduction of continental crust and topography.

The pressure and temperature fields computed from the model can be used to calculate the distribution of density based on the initial rock composition within each different domain (table 1). Our approach follows the procedures proposed by [Bousquet, *et al.*, 1997] and accounts for compressibility and thermal expansion of the materials (table 1). One of the assumptions behind these calculations is that mineral assemblages have attained thermodynamic equilibrium independently of the P-T-t history and of the kinetics of the reactions; this might be questioned however in the case of Taiwan. Results are illustrated in figure 17 and show that the distribution of densities is roughly controlled by the thermal structure. Densities exceeding ~ 3 are found within the underthrust crust below the orogenic wedge due to its gradual increase in density with depth. As a result, the density contrast between the downgoing crust and the mantle decreases progressively in the direction of subduction. This might explain the absence of a high topography (figure 17) as well as of a clear seismic Moho east of the central range [Kim, *et al.*, 2005; Lin, 2005; McIntosh, *et al.*, 2005; Shih, *et al.*, 1998; Yeh, *et al.*, 1998]. The possibility that dense crust would be subducted and the fact that it would generally correspond with a poorly seismically defined Moho has already been pointed out for some other examples of collisional orogens [Bousquet, *et al.*, 1997; Goffe, *et al.*, 2003; Le Pichon, *et al.*, 1997]. These results are thus consistent with the thermo-kinematics previously proposed since they allow for subduction of the continental crust not incorporated into the prism. More precisely, the density increases not only within the lower crust of the Chinese margin, but also within the fraction of the upper crust not involved in the orogenic wedge (figure 17a).

Details in the distribution of computed densities inside the wedge are shown in figure 17b, and seem also essentially controlled by the thermal structure. Interestingly, a low in density is predicted beneath the BR, at depths of ~ 10 km and for temperatures of 200 to 300 °C. This is because at these particular pressure and temperature conditions, thermal expansion prevails over compressibility as illustrated in the petrogenetic grid shown on figure 1b of [Bousquet, *et al.*, 2005], although this latter case has been derived for more mafic compositions. From the density field, we also computed the topography that should result in the case of local isostasy, assuming compensation in the asthenosphere. The details of the procedures are already described in other papers [Bousquet, *et al.*, 1997; Goffe, *et al.*, 2003; Henry, *et al.*, 1997]. This simple approach is able to reproduce the overall topography (figure 17c). Indeed, the predicted low in density would explain the location of the highest elevations over the BR, as well as the lower topography

over the underplating windows below the more metamorphic HR and TC on either side. In fact, the real topography should exceed the one predicted from this model because of the flexural support of the range [Lin and Watts, 2002]. This example confirms that the density distribution resulting from metamorphism within an orogenic wedge may have significant effects on the topography and morphology of the range (e.g. [Goffe, et al., 2003]). Such parameters ought to be taken into account in mechanical models of mountain-building.

5.4 Re-appraisal of mountain-building processes in Taiwan.

The case of Taiwan has been key in the development of the popular critical wedge theory for mountain-building [Barr and Dahlen, 1989; Barr, et al., 1991; Dahlen and Barr, 1989; Davis, et al., 1983]. It turns out that the initial model does not account well for the thermometric and thermo-chronological data that are now available (e.g. [Beysac, et al., in prep.]) (figure 2). Also, it seems that the range in Taiwan does not experience the distributed shortening that we would expect for an eroding critical wedge. Our analysis indicates that the overall structural architecture, and metamorphic history of the orogen can be successfully accounted for by assuming that the shortening across the range is totally taken up by major structures at the front; no internal deformation, possibly resulting from out-of sequence thrusting within the wedge as proposed by [Tillman and Byrne, 1996], is in fact required. In our model, underplating may contribute to as much as ~ 90% of the incoming flux of rocks into the wedge (~ 20 % below HR and 70 % beneath TC); major changes in fact occurred ~1.5 Ma ago with the widening of the underplating window over TC, but also, to another extent, ~ 4 Myr ago (in the case of the northern transect; figure 11) with initiation of HR. This is much more than the maximum value of 25% estimated by [Barr and Dahlen, 1989; Barr, et al., 1991; Dahlen and Barr, 1989]. It is possible that underplating and surface processes act together to maintain a range topography that is always overcritical so that the deviatoric stresses within the wedge remain too small to induce internal deformation.

In addition to that, by integrating the spatio-temporal evolution of the range as derived from the foreland basin [Simoes and Avouac, in prep.], as well as the whole metamorphic history of the rocks from their peak temperature to their cooling up to the surface, we found major changes in the mode of growth of the orogen, challenging the idea of a steady-state wedge.

6. Conclusion

The spatio-temporal evolution of the Taiwanese range has been re-appraised in light of the kinematics of deformation derived by [Simoes and Avouac, in prep.], as well as the available thermometric and thermo-chronological data (e.g. [Beyssac, et al., in prep.; Liu, et al., 2001; Lo and Onstott, 1995; Tsao, 1996; Willett, et al., 2003]). All these diverse constraints may all be successfully reconciled in a simple thermo-kinematic model where the wedge is not submitted to any internal shortening; this view contrasts with the critical wedge theory applied to the Taiwan orogen by [Barr and Dahlen, 1989; Barr, et al., 1991; Dahlen and Barr, 1989], which seems unable to account for exhumation of the HR. Our findings also indicate that frontal accretion has contributed to most of the orogenic growth at initial stages, but that the wedge is presently thickening essentially as a result of underplating below the TC and HR. The balance of incoming and outgoing fluxes requires a large amount of crustal subduction, probably allowed by the increase in density of the downgoing crust. Metamorphic changes and the influence of surface processes on the thermal structure and stress redistribution appear to be key factors to explain the dynamics of mountain building. This study sheds new light on mountain-building processes in the case of this young arc-continent collision zone.

Acknowledgements

M.S. wishes to thank P. Henry (CEREGE, France) and L. Bollinger (CEA, France) for introducing her to the FEAP program used in modeling the evolution of the Taiwanese orogen; this code has been developed by R. Taylor of U.C. Berkeley. Heat flow data were kindly provided by K.-F. Ma (NCU, Taiwan) and T.-R. A. Song (Caltech, CA); Y.-J Hsu and J. Giberson (Caltech, CA) also helped access the seismicity data from the CWB catalog. The modeling presented in this paper benefited from discussions on the data with G. Maheo (Universite Lyon1, France).

References

- Avouac, J. P. (2003), Mountain building, erosion and the seismic cycle in the Nepal Himalaya., in *Advances in Geophysics.*, edited by R. Dmowska, Elsevier, Amsterdam.
- Avouac, J. P., and E. B. Burov (1996), Erosion as a driving mechanism of intracontinental mountain growth., *Journal of Geophysical Research*, *101*, 17747-17769.
- Barr, T. D., and F. A. Dahlen (1989), Brittle frictional mountain building 2. Thermal structure and heat budget., *Journal of Geophysical Research*, *94*, 3923-3947.
- Barr, T. D., F. A. Dahlen, and D. C. McPhail (1991), Brittle frictional mountain building 3. Low-grade metamorphism., *Journal of Geophysical Research*, *96*, 10319-10338.

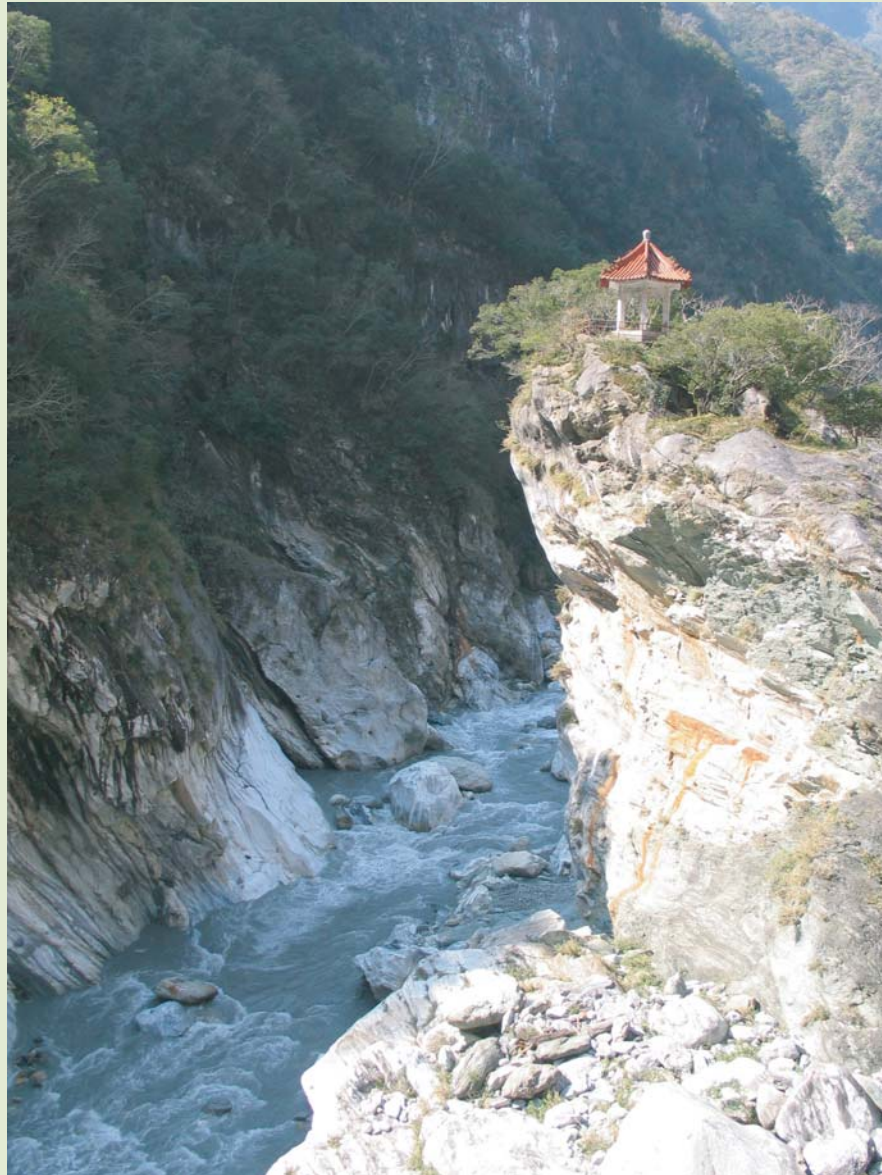
- Beaumont, C., P. Fullsack, and J. Hamilton (1992), Erosional control of active compressional orogens., in *Thrust Tectonics*, edited by K. R. McClay, pp. 19-31, Chapman & Hall, New York.
- Beyssac, O., J. P. Avouac, M. Simoes, K. A. Farley, Y.-G. Chen, Y.-C. Chan, and B. Goffe (in prep.), Thermal and thermochronological constraints on the late Cenozoic metamorphic evolution and exhumation of Taiwan., *for: Journal of Geophysical Research*.
- Beyssac, O., B. Goffe, C. Chopin, and J.-N. Rouzaud (2002), Raman spectra of carbonaceous material in metasediments: a new geothermometer., *Journal of Metamorphic Geology*, 20, 859-871.
- Bollinger, L., J. P. Avouac, O. Beyssac, E. J. Catlos, T. M. Harrison, M. Grove, B. Goffe, and S. Sapkota (2004a), Thermal structure and exhumation history of the Lesser Himalaya in Central Nepal, *Tectonics*, 23, doi:10.1029/2003TC001564.
- Bollinger, L., J. P. Avouac, R. Cattin, and M. R. Pandey (2004b), Stress buildup in the Himalaya, *Journal of Geophysical Research*, 109, doi:10.1029/2003JB002911.
- Bollinger, L., P. Henry, and J. P. Avouac (subm.), Mountain building in the Nepal Himalaya: thermal and kinematic model., *Earth and Planetary Science Letters*.
- Bos, A. G., W. Spakman, and M. C. J. Nyst (2003), Surface deformation and tectonic setting of Taiwan inferred from a GPS velocity field., *J. Asian Earth Sci.*, 108, 2458.
- Bousquet, R., B. Goffe, P. Henry, X. Le Pichon, and C. Chopin (1997), Kinematic, thermal and petrological model of the Central Alps: Lepontine metamorphism in the upper crust and eclogitisation of the lower crust., *Tectonophysics*, 273, 105-127.
- Bousquet, R., B. Goffe, X. Le Pichon, C. De Capitani, C. Chopin, and P. Henry (2005), Comment on "Subduction factory: 1. Theoretical mineralogy, densities, seismic wave speeds, and H₂O contents" by Bradely R. Hacker, Geoffrey A. Abers, and Simon M. Peacock., *Journal of Geophysical Research*, 110, 10.1029:2004JB003450.
- Byrne, T. B., and C.-S. Liu (2002), Introduction to the geology and geophysics of Taiwan, in *Geology and geophysics of an arc-continent collision, Taiwan.*, edited by T. B. Byrne and C.-S. Liu, pp. V-VIII, Geological Society of America Special Paper, Boulder, CO, USA.
- Carena, S., J. Suppe, and H. Kao (2002), Active detachment of Taiwan illuminated by small earthquakes and its control of first-order topography., *Geology*, 30, 935-938.
- Cattin, R., and J. P. Avouac (2000), Modeling mountain building and the seismic cycle in the Himalaya of Nepal, *Journal of Geophysical Research*, 105, 13389-13407.
- Chang, H. C. (1989), Radioactivity and heat generation of rocks in the Taiwan region., PhD thesis, 159 pp, National Central University, Chung-Li.
- Chapple, W. M. (1978), Mechanics of thin-skinned fold-and-thrust belts, *Geological Society of America Bulletin*, 89, 1189-1198.
- Clark, M. B., D. M. Fisher, C.-Y. Lu, and C.-H. Chen (1993), Kinematic analyses of the Hsueshan range, Taiwan: a large-scale pop-up structure., *Tectonics*, 12, 205-217.
- Crespi, J. M., Y.-C. Chan, and M. S. Swaim (1996), Synorogenic extension and exhumation of the Taiwan hinterland., *Geology*, 24, 247-250.
- Dadson, S. J., N. Hovius, H. Chen, W. B. Dade, M.-L. Hsieh, S. D. Willett, J.-C. Hu, M.-J. Horng, M.-C. Chen, C. P. Stark, D. Lague, and J. C. Lin (2003), Links between erosion, runoff variability and seismicity in the Taiwan orogen., *Nature*, 426, 648-651.
- Dahlen, F. A., and T. D. Barr (1989), Brittle frictional mountain building 1. Deformation and mechanical energy budget., *Journal of Geophysical Research*, 94, 3906-3922.
- Davis, D., J. Suppe, and F. A. Dahlen (1983), Mechanics of fold-and-thrust belts and accretionary wedges., *Journal of Geophysical Research*, 88, 1153-1172.
- Dorsey, R. J., and N. Lundberg (1988), Lithofacies analysis and basin reconstruction of the Plio-Pleistocene collisional basin, Coastal Range of Eastern Taiwan., *Acta Geologica Taiwanica*, 26, 57-132.
- Ernst, W. G. (1983), Mineral paragenesis in metamorphic rocks exposed along Tailuko Gorge, Central Mountain-range, Taiwan, *J. Metam. Geol.*, 1, 305-329.
- Ernst, W. G., and B. M. Jahn (1987), Crustal accretion and metamorphism in Taiwan, a post-Paleozoic mobile belt., *Philosophical Transactions of the Royal Society of London.*, A321, 129-161.
- Faure, M., C. Y. Lu, and H. T. Chu (1991), Ductile deformation and Miocene nappe-stacking in Taiwan related to motion of the Philippine Sea Plate., *Tectonophysics*, 198, 95-105.
- Fisher, D. M., C. Y. Lu, and H. T. Chu (2002), Taiwan Slate Belt: insights into the ductile interior of an arc-continent collision., in *Geology and geophysics of an arc-continent collision, Taiwan.*, edited by T. B. Byrne and C.-S. Liu, pp. 93-106, Geological Society of America., Boulder.
- Godard, V., R. Cattin, and J. Lave (2004), Numerical modeling of mountain building: interplay between erosion law and crustal rheology, *Geophysical Research Letters*, 31, doi:10.1029/2004GL021006.

- Goffe, B., R. Bousquet, P. Henry, and X. Le Pichon (2003), Effect of the chemical composition of the crust on the metamorphic evolution of orogenic wedges., *Journal of Metamorphic Geology*, 21, 123-141.
- Gourley, J. R., T. Byrne, F. T. Wu, Y.-C. Chan, and S. Yu (2004), Along strike GPS and seismic constraints on extension in eastern Central Range, paper presented at AGU Fall Meeting, San Francisco, CA.
- Hansen, F. D., and N. L. Carter (1982), Creep of selected crustal rocks at 1000 MPa., *EOS, Transactions, American Geophysical Union*, 63, 437.
- Henry, P., X. Le Pichon, and B. Goffe (1997), Kinematic, thermal and petrological model of the Himalayas; constraints related to metamorphism within the underthrust Indian crust and topographic elevation., *Tectonophysics*, 273, 31-56.
- Hickman, J. B., D. V. Wiltschko, J.-H. Hung, P. Fang, and Y. Bock (2002), Structure and evolution of the active fold-and-thrust belt of Southwestern Taiwan from Global Positioning System analysis., *Geological Society of America Special Paper*, 358, 75-92.
- Ho, C. S. (1986), A synthesis of the geologic evolution of Taiwan., *Tectonophysics*, 125, 1-16.
- Ho, C. S. (1988), *An introduction to the geology of Taiwan - Explanatory text of the geologic map of Taiwan*, second ed., 192 pp., Central Geological Survey, Taipei, ROC.
- Huerta, A. D., L. H. Royden, and K. V. Hodges (1998), The thermal structure of collisional orogens as a response to accretion, erosion, and radiogenic heating., *Journal of Geophysical Research*, 103, 15287-15302.
- Hung, J.-H., D. V. Wiltschko, H.-C. Lin, J. B. Hickman, P. Fang, and Y. Bock (1999), Structure and motion of the southwestern Taiwan fold and thrust belt., *Terr. Atmos. Ocean. Sci.*, 10, 543-568.
- Hwang, W.-T., and C.-Y. Wang (1993), Sequential thrusting model for mountain building: constraints from geology and heat flow of Taiwan., *Journal of Geophysical Research*, 98, 9963-9973.
- Kim, K.-H., J.-M. Chiu, J. Pujol, K. C. Chen, B. S. Huang, Y. H. Yeh, and P. Shen (2005), Three-dimensional Vp and Vs structural models associated with the active subduction and collision tectonics in the Taiwan region., *Geophysical Journal International*, 162, 204-220.
- Koons, P. O. (1990), Two-sided orogen: collision and erosion from the sandbox to the Southern Alps, New Zealand., *Geology*, 18, 679-682.
- Koons, P. O., P. K. Zeitler, C. P. Chamberlain, D. Craw, and A. S. Meltzer (2002), Mechanical links between erosion and metamorphism in Nanga Parbat, Pakistan Himalaya., *Am. J. Sci.*, 302, 749-773.
- Kuochen, H., Y. Wu, Y. Chen, R. Chen, and Y. Kuo (2004), Seismogenic structures in Hualien region, Eastern Taiwan., paper presented at AGU Fall Meeting, American Geophysical Union, San Francisco, CA.
- Le Pichon, X., P. Henry, and B. Goffe (1997), Uplift of Tibet: from eclogites to granulites - implications for the Andean plateau and the Variscan belt, *Tectonophysics*, 273, 57-76.
- Lee, C. R., and W. T. Cheng (1986), Preliminary heat flow measurements in Taiwan, paper presented at Fourth Circum-Pacific Energy And Mineral Resources Conference, Singapore.
- Lee, J.-C., J. Angelier, and H. T. Chu (1997), Polyphase history and kinematics of a complex major fault zone in the northern Taiwan mountain belt: the Lishan fault., *Tectonophysics*, 274, 97-115.
- Lin, A. T., and A. B. Watts (2002), Origin of the West Taiwan basin by orogenic loading and flexure of a rifted continental margin., *Journal of Geophysical Research*, 107 (B9), doi:10.129/2001JB000669.
- Lin, A. T., A. B. Watts, and S. P. Hesselbo (2003), Cenozoic stratigraphy and subsidence history of the South China Sea margin in the Taiwan region., *Basin Research*, 15, 453-478.
- Lin, C.-H. (2000), Thermal modeling of continental subduction and exhumation constrained by heat flow and seismicity in Taiwan., *Tectonophysics*, 324, 189-201.
- Lin, C. H. (1998), Tectonic implications of an aseismic belt beneath Eastern Central range of Taiwan: crustal subduction and exhumation., *Journal of the Geological Society of China.*, 41, 441-460.
- Lin, C. H. (2005), Identification of mantle reflections from a dense linear seismic array: tectonic implications to the Taiwan orogeny., *Geophysical Research Letters*, 32, doi:10.1029/2004GL021814.
- Liou, J. G., C. O. Ho, and T. P. Yen (1975), Petrology of some glaucophane schists and related rocks from Taiwan., *Journal of Petrology*, 16, 80-109.
- Liu, T.-K. (1982), Tectonic implications of fission track ages from the Central Range, Taiwan., *Proceedings of the Geological Society of China.*, 25, 22-37.
- Liu, T.-K., S. Hsieh, Y.-G. Chen, and W.-S. Chen (2001), Thermo-kinematic evolution of the Taiwan oblique-collision mountain belt as revealed by zircon fission-track dating., *Earth and Planetary Science Letters*, 186, 45-56.
- Lo, C.-H., and T. C. Onstott (1995), Rejuvenation of K-Ar systems for minerals in the Taiwan mountain belt., *Earth and Planetary Science Letters*, 131, 71-98.
- Lo, C.-H., and T.-F. Yui (1996), ⁴⁰Ar/³⁹Ar dating of high-pressure rocks in the Tananao basement complex, Taiwan, *Journal of the Geological Society of China.*, 39, 13-30.

- McIntosh, K., Y. Nakamura, T.-K. Wang, R. C. Shih, A. Chen, and C. S. Liu (2005), Crustal-scale seismic profiles across Taiwan and the Western Philippine Sea., *Tectonophysics*, 401, 23-54.
- Mouthereau, F., O. Lacombe, B. Deffontaines, J. Angelier, and S. Brusset (2001), Deformation history of the southwestern Taiwan foreland thrust belt: insights from tectono-sedimentary analyses and balanced cross-sections., *Tectonophysics*, 333, 293-322.
- Powell, L. K. (2003), Feedback between erosion and fault reactivation in the Puli Basin: Hsueshan belt of Central Taiwan., Master thesis, 61 pp, University of Colorado.
- Pulver, M. H., J. M. Crespi, and T. B. Byrne (2002), Lateral extrusion in a transpressional collision zone: an example from the pre-Tertiary metamorphic basement of Taiwan., in *Geology and Geophysics of an arc-continent collision, Taiwan.*, edited by T. B. Byrne and C. S. Liu, pp. 107-120, Geological Society of America Special Paper, Boulder, CO, USA.
- Rao, C. T., and P. L. Li (1994), Heat flow in the Zhujiangkou Basin, *Oil Eastern South China Sea.*, (in Chinese with English abstract), 10-18.
- Reiners, P. W., T. L. Spell, S. Nicolescu, and K. A. Zanetti (2004), Zircon (U-Th)/He thermochronometry; He diffusion and comparisons with (super 40) Ar/ (super 39)Ar dating, *Geochimica and Cosmochimica Acta*, 68, 1857-1887.
- Sella, G. F., T. H. Dixon, and A. Mao (2002), REVEL: a model for recent plate velocities from space geodesy., *Journal of Geophysical Research*, 107, 2081.
- Seno, T., and S. Maruyama (1984), Paleogeographic reconstruction and origin of the Philippine Sea, *Tectonophysics*, 102, 53-84.
- Shackleton, N. J., J. Imbrie, and N. G. Pisias (1988), The evolution of oceanic oxygen-isotope variability in the North Atlantic over the past three million years., *Philosophical Transactions of the Royal Society of London.*, B318, 679-688.
- Shih, R. C., C. H. Lin, H. L. Lai, Y. H. Yeh, B. S. Huang, and H. Y. Yen (1998), Preliminary crustal structures across Central Taiwan from modeling of the onshore/offshore wide-angle seismic data., *Terr. Atmos. Ocean. Sci.*, 9, 317-328.
- Simoes, M., and J. P. Avouac (in prep.), Investigating the kinematics of mountain-building in Taiwan, from the spatio-temporal evolution of the foreland basin and foothills., *for: Journal of Geophysical Research*.
- Song, A. T.-R., and K.-F. Ma (2002), Estimation of the thermal structure of a young orogenic belt according to a model of whole-crust thickening., in *Geology and geophysics of an arc-continent collision, Taiwan.*, edited by T. B. Byrne and C. S. Liu, pp. 121-136, Geological Society of America Special Paper, Boulder, CO, USA.
- Suppe, J. (1980a), Imbricated structure of Western Foothills Belt, Southcentral Taiwan., *Petroleum Geology of Taiwan.*, 17, 1-16.
- Suppe, J. (1980b), A retrodeformable cross section of Northern Taiwan., *Proceedings of the Geological Society of China.*, 23, 46-55.
- Suppe, J. (1981), Mechanics of mountain building and metamorphism in Taiwan., *Memoir of the Geological Society of China.*, 4, 67-89.
- Suppe, J. (1984), Kinematics of arc-continent collision, flipping of subduction, and back-arc spreading near Taiwan., *Memoir of the Geological Society of China.*, 6, 21-33.
- Suppe, J. (1987), The active Taiwan mountain belt., in *The anatomy of mountain ranges.*, edited by J.-P. Schaer and J. Rodgers, pp. 277-293, Princeton University Press., Princeton, New Jersey, USA.
- Taylor, S. M., and S. M. McLennan (1985), *The continental crust: its composition and evolution.*, Blackwell, Oxford, UK.
- Teng, L. S. (1990), Geotectonic evolution of late Cenozoic arc-continent collision in Taiwan., *Tectonophysics*, 183, 57-76.
- Tillman, K. S., and T. B. Byrne (1995), Kinematic analysis of the Taiwan Slate Belt., *Tectonics*, 14, 322-341.
- Tillman, K. S., and T. B. Byrne (1996), Out-of-sequence thrusting in the Taiwan slate belt., *Journal of the Geological Society of China.*, 39, 189-208.
- Tsao, S. J. (1996), The geological significance of illite crystallinity, zircon fission-track ages and K-Ar ages of metasedimentary rocks of the Central Range., PhD thesis, 272 pp, National Taiwan University, Taipei, Taiwan.
- Turcotte, D. L., and G. Schubert (2002), *Geodynamics - 2nd Edition*, 2nd ed., 456 pp., Cambridge University Press, Cambridge, UK.
- Willett, S. D. (1999), Orogeny and topography: the effects of erosion on the structure of mountain belts., *Journal of Geophysical Research*, 104, 28957-28981.
- Willett, S. D., C. Beaumont, and P. Fullsack (1993), Mechanical model for the tectonics of doubly vergent compressional orogens, *Geology*, 21, 371-374.
- Willett, S. D., D. M. Fisher, C. W. Fuller, Y. En-Chao, and L. Chia-Yu (2003), Erosion rates and orogenic-wedge kinematics in Taiwan inferred from fission-track thermochronometry., *Geology*, 31, 945-948.
- Yeh, Y. H., R. C. Shih, C. W. Lin, C. C. Liu, H. Y. Yen, B. S. Huang, C. S. Liu, P. Z. Chen, C. S. Huang, C. J. Wu, and F. T. Wu (1998), Onshore/offshore wide-angle deep seismic profiling in Taiwan., *Terr. Atmos. Ocean. Sci.*, 9, 301-316.

- Yen, H. Y., Y. H. Yeh, and F. T. Wu (1998), Two-dimensional crustal structures of Taiwan from gravity data, *Tectonics*, 17, 104-111.
- Yue, L.-F., J. Suppe, and J.-H. Hung (2005), Structural geology of a classic thrust belt earthquake: the 1999 Chi-Chi earthquake Taiwan (Mw=7.6), *Journal of Structural Geology*, 27, 2058-2083.
- Zeitler, P. K., P. O. Koons, M. Bishop, C. P. Chamberlain, D. Craw, M. A. Edwards, S. Hamidullah, M. Q. Jan, M. A. Khan, M. U. Khan Khattak, W. S. F. Kidd, R. L. Mackie, A. S. Meltzer, S. K. Park, A. Pecher, M. A. Poage, G. Sarker, D. A. Schneider, L. Seeber, and J. Shroder (2001), Crustal reworking at the Nanga Parbat, Pakistan: metamorphic consequences of thermal-mechanical coupling facilitated by erosion., *Tectonics*, 20, 712-728.
- Zhou, D., H.-S. Yu, H.-H. Xu, X.-B. Shi, and Y.-W. Chou (2003), Modeling of thermo-rheological structure of lithosphere under the foreland basin and mountain belt of Taiwan., *Tectonophysics*, 374, 115-134.
- Zienkiewicz, O. C., and R. L. Taylor (1989), *The finite-element method.*, McGraw-Hill, New York, NY.

Chapter 4:
*Conclusion and perspectives
for future research*



Taroko Gorge, eastern Taiwan

